



The Open Civil Engineering Journal

Content list available at: <https://opencivilengineeringjournal.com>



RESEARCH ARTICLE

Seismic Retrofit of an Existing Reinforced Concrete Building with Buckling-restrained Braces

Massimiliano Ferraioli^{1,*}, Angelo Lavino¹, Carmine Moliterno² and Gennaro Di Lauro¹

¹Department of Engineering (DI), Università della Campania "Luigi Vanvitelli" Via Roma 9, 81031, Aversa, Italy

²Department of Structures for Engineering and Architecture, Università di Napoli "Federico II" Via Claudio 21, 80125, Napoli, Italy

Abstract:

Background:

The seismic retrofitting of frame structures using hysteretic dampers is a very effective strategy to mitigate earthquake-induced risks. However, its application in current practice is rather limited since simple and efficient design methods are still lacking, and the more accurate time-history analysis is time-consuming and computationally demanding.

Aims:

This paper develops and applies a seismic retrofit design method to a complex real case study: An eight-story reinforced concrete residential building equipped with buckling-restrained braces.

Methods:

The design method permits the peak seismic response to be predicted, as well as the dampers to be added in the structure to obtain a uniform distribution of the ductility demand. For that purpose, a pushover analysis with the first mode load pattern is carried out. The corresponding story pushover curves are first idealized using a degrading trilinear model and then used to define the SDOF (Single Degree-of-Freedom) system equivalent to the RC frame. The SDOF system, equivalent to the damped braces, is designed to meet performance criteria based on a target drift angle. An optimal damper distribution rule is used to distribute the damped braces along the elevation to maximize the use of all dampers and obtain a uniform distribution of the ductility demand.

Results:

The effectiveness of the seismic retrofit is finally demonstrated by non-linear time-history analysis using a set of earthquake ground motions with various hazard levels.

Conclusion:

The results proved the design procedure is feasible and effective since it achieves the performance objectives of damage control in structural members and uniform ductility demand in dampers.

Keywords: Reinforced concrete buildings, Seismic retrofit, Hysteretic dampers, Nonlinear time-history analysis, Buckling-restrained braces, SDOF system.

Article History

Received: October 17, 2020

Revised: November 20, 2020

Accepted: December 9, 2020

1. INTRODUCTION

Many existing buildings in high seismicity regions were designed and constructed without any design provision for earthquake resistance. In these buildings, seismic energy is dis-

sipated by the plastic deformations of the structural elements, which cause performance deterioration and damage. Among possible retrofit strategies, the approach involving both stiffness and strength increments has been the most commonly used one over the past decades. The main drawback of this approach is that it increases not only the strength but also the lateral stiffness of the building, thus resulting in higher seismic actions. As an alternative, the concept of passive control

* Address correspondence to this author at Department of Engineering (DI), Università della Campania "Luigi Vanvitelli" Via Roma 9, 81031, Aversa, Italy; Tel: 0815010210; E-mail: massimiliano.ferraioli@unicampania.it

strategies based on energy dissipation devices has been significantly developed in recent years [1, 2]. Various types of energy dissipation devices are currently used for the seismic retrofit of reinforced concrete (RC) buildings. Among them, various types of metallic yielding dampers have been developed that use both the plastic deformation capacity and the ductility of hysteretic materials (such as mild steel, aluminum, or shape memory alloys) to dissipate seismic energy [3 - 10]. These dampers are classified based on the yielding mechanism (*i.e.*, axial dampers, yielding ring dampers, extrusion devices, torsional bar dampers, and shear panel dampers) and used with various configurations (*i.e.*, brace type, wall panel type, stud panel type, and shear link panel type). Nowadays, the elasto-plastic (EP) axial steel dampers are extensively used in diagonal braces for the seismic energy dissipation (*i.e.*, buckling restrained braces) since they significantly decrease both member forces and inter-story drifts under earthquake ground motion. However, their practical design is more complex than other retrofit strategies since they significantly modify both stiffness and damping characteristics of the structure. The increase in lateral stiffness shortens the natural periods of vibration, and this usually increases the acceleration demand. The increase in damping increases the energy dissipation capacity of the structure. Additionally, when the damper yields, often the whole structure loses the lateral stiffness of one story, with the consequent failure due to the development of a soft story mechanism. The design procedure should account for the hysteretic behavior of both the dampers and the RC members and include their interaction under earthquake ground motion. Hence the lack of efficient design methods in the literature, as well as of standardized design procedures in the seismic codes. The application of conventional methods (such as the traditional force-based “R-Factor method” as prescribed in SEI/ASCE 7-05 [11] or the “q-factor method” as suggested in Eurocode 8 [12]) to RC damped braced buildings becomes prohibitively difficult. In fact, due to the lack of stable relationships among damping, response reduction factors, and earthquake ground motion, the behavior factor is difficult to obtain accurately.

On the other side, the application in the current practice of more sophisticated methods, such as the non-linear time-history analysis, is relatively small because it involves many additional data (*i.e.*, accurate hysteretic models and spectrum compatible earthquake records) and requires advanced modeling and computationally intensive analyses. Hence, several methods directed at improving and simplifying the design phase were available in the literature. For example, Foraboschi [13] proposed a simple formula that blends plastic analysis and non-linear analysis to investigate the ultimate behavior of RC structures and developed a predictive formulation for the ultimate combination of axial force and bending moment for steel members [14]. As an alternative to non-linear dynamic analysis, many seismic design procedures have been proposed in the literature [15 - 22] and implemented in current design codes [23 - 25]. The state-of-the-art review shows that many of these design methods combine the Displacement-Based Design (DBD) and the proportional stiffness criterion. In this approach, the distribution of the lateral loads on the damped braces is considered proportional

to the first mode shape. This hypothesis is assumed to be true in the case of regular structures where the mode shapes remain practically unchanged after retrofitting. However, it fails in many existing RC buildings since they are often irregular in-plan or elevation and may exhibit a poor seismic behavior (*e.g.*, lateral-torsional coupling effects, soft-story mechanisms, and non-ductile columns). Other studies [26 - 30] proposed damper optimization methods, aiming to obtain uniform ductility demand distributions. However, these methods are generally developed based on simplified shear beam models, while applications to complex multi-story buildings are still lacking. Thus, it is desirable for the development of simple and more practical design procedures and their application to real case studies and, particularly, to schools, hospitals, and other public buildings, considering their importance due to the consequences associated with their failure [31 - 33]. This paper presents an interesting application of a seismic retrofit design method to an existing reinforced concrete building using Buckling-Restrained Braces (BRBs). The design procedure aims to predict the peak seismic response and arrange dampers to attain a uniform distribution of the ductility demand. For this purpose, a comprehensive design method is developed and applied to address the main issues of the seismic design of damped braces, *i.e.*, complex hysteretic behavior of RC structural members, frame-damped braces interaction, and effect of non-uniform displacement demands and partial collapse mechanisms. Its effectiveness is finally investigated through non-linear response history analyses considering suites of earthquake ground motion records representing different seismic hazard levels.

2. REVIEW OF RETROFIT DESIGN METHODS FOR RC BUILDINGS USING HYSTERETIC DAMPERS

The seismic design standards of several countries apply the energy dissipation concept, and some current design codes [24 - 26] have developed design principles for the damped structures, including analytical models for the dampers and methods of analysis for the seismic response. In general, the coefficient method based on FEMA 273 [34] and the capacity-spectrum method based on ATC-40 [35] have given rise to two different approaches, one founded on the Direct Displacement-Based Design method (DDBD) and the other based on the Capacity-Spectrum Method (CSM). The design method proposed by the Japan Society of Seismic Isolation [36] applies the so-called elastic response reduction curve. This approach neglects the inelastic behavior of the main structure, thus overestimating the reduction in acceleration. To overcome this limitation, Shen *et al.* [37] proposed a simple design method based on the Elastic-Plastic Response Reduction Curve (EPRRC). Lee and Kim [38] developed a design procedure based on the capacity spectrum method for the seismic retrofit of an existing reinforced concrete building with steel slit dampers. Lin *et al.* [18] presented a seismic displacement-based design method and provided the effective viscous damping ratio for various passive energy dissipation devices. Kim *et al.* [39] proposed a direct displacement design procedure for steel frames with buckling-restrained braces. Teran-Gilmorea *et al.* [40] introduced a displacement-based methodology for the preliminary design of buckling-restrained

braces, neglecting both the higher modes and the torsional effects. Since damage is related to both the maximum displacement and the energy dissipated during the earthquake, various energy-based design methods are available in the literature. Kim *et al.* [41] proposed a simplified design procedure based on the energy balance concept and equal energy dissipation. Choi *et al.* [42] presented an energy-based seismic design procedure for framed structures with buckling-restrained braces using hysteretic energy spectra and accumulated ductility spectra. Habibi *et al.* [43] developed a step-wise multi-mode energy-based design method for seismic retrofitting of frame structures with energy dissipative devices. Recently, optimal design methods aim to define the locations and sizes of the devices to obtain the best performance at a lower cost. Miguel *et al.* [44] proposed a robust design optimization based on two objective functions and a genetic algorithm that is applied to solve the resulting multi-objective optimization problem. As an alternative to such genetic algorithms, Martínez *et al.* [45] proposed a stochastic equivalent linearization to optimally define the energy dissipation capacity of added non-linear hysteretic dampers. Terazawa *et al.* [46] presented a damper design routine for highly indeterminate 3D structures utilizing computational optimization and response spectrum analysis. However, all these methods have important limitations since they are time-consuming and computationally demanding, especially when applied to complex buildings. Furthermore, results may vary significantly with different earthquake ground motions. Finally, many of these design methods base on steel structures, where the beam-column brace connections are pinned, and the damped braces resist all the lateral seismic forces. Many other studies neglect the real nature of the building after retrofit that is a dual system (bare frame plus dissipating braces) with a not negligible frame-damped brace interaction. Mazza *et al.* [21] proposed a design procedure that arranges the dampers according to the fundamental mode based on the Displacement-Based Design (DBD) and the proportional stiffness criterion. The SDOF system, equivalent to the existing building, and the SDOF system, equivalent to the damped braces, were considered separately, thus neglecting the frame-damped brace interaction. Moreover, the RC frame contribution to the pushover capacity of the building depends on the non-linear response of the structure that may be significantly modified by the addition of the damped braces. To overcome these limitations, Ferraioli and Lavino [22] developed a displacement-based design method based on the adaptive pushover analysis that explicitly accounts for the frame-damped brace interaction. Other studies [26 - 30, 36] proposed a closed-form formula for the damper-frame stiffness ratio and a rule to distribute the damper stiffness over the height of the structure. However, both methodological and practical problems limit their application in the current practice. This approach bases on two-dimensional planar shear-bar models. Thus, it is fully reliable only when applied to symmetric-in-plan buildings with a first-mode dominant response. On the contrary, many existing RC buildings are asymmetric in-plan or irregular in elevation. Thus, their seismic response is significantly affected by the lateral-torsional coupling and the higher modes contribution producing non-uniform displacement demands and partial collapse mechanisms. Moreover, this approach may give

inconsistent results for both “upper-deformed type” frames and “lower-deformed type” frames. When applied to “upper-deformed type” frames (*i.e.*, frames where the drift at upper stories increases), this approach provides that no damped brace is necessary for the first story. This design solution would produce a brittle mechanism due to the shear failure of the columns. When applied to “lower-deformed type” frames (*i.e.*, frames where the drift at lower stories increases), this approach could provide a negative stiffness for the damped braces at the upper stories. This negative value means that the story stiffness of the RC frame at the upper stories is too high, thus preventing the yielding of the damped braces. Therefore, more developments and applications to complex buildings are necessary to address the main issues involved in the implementation of efficient retrofit design procedures.

3. MATERIALS AND METHODS

3.1. Retrofit Design Method

3.1.1. Pushover Analysis and Trilinear Idealization of the Story Pushover Curves

The design procedure bases on decomposing the structural system into two subsystems: the frame system and the damped brace system (Fig. 1). Each subsystem is idealized using first a simplified MDOF model, and then an equivalent SDOF system (Figs. 2-3). The SDOF system, equivalent to the RC frame, is defined based on the pushover analysis using the first mode distribution of lateral forces. The corresponding story pushover curves are plotted in Fig. (4a). Each story pushover curve is then idealized using a degrading trilinear behavior following the Takeda model [47]. The parameters of the trilinear idealization of the pushover curve for the i -th story are shown in Fig. (5), where:

- $K_{0,i}^f$, $\alpha_1 K_{0,i}^f$ and $\alpha_2 K_{0,i}^f$ are the elastic, post-crack, and post-yield stiffness;
- $V_{y,i}^f$, $\delta_{y,i}^f$ and $K_{y,i}^f$ are the shear force, the inter-story displacement, and the secant stiffness at yielding;
- $V_{c,i}^f$ and $\delta_{c,i}^f$ are the shear force and the inter-story displacement corresponding to cracking of concrete;
- $\delta_i^f = \mu_i^f \delta_{y,i}^f$ and $K_{\mu,i}^f$ are the maximum inter-story displacement and the corresponding secant stiffness.

To calculate these parameters, in this paper the following hypotheses are made:

- 1) the elastic stiffness $K_{0,i}^f$ is calculated as the tangent stiffness of the pushover curve;
- 2) the post-yield stiffness is assumed to be zero (*i.e.*, $\alpha_2 = 0$);

Under these hypotheses, the yielding displacement $\delta_{y,i}^f$ is the only unknown parameter of the problem. Sutcu *et al.* [5] used the condition $\mu_{c,i}^f = \delta_{c,i}^f / \delta_{y,i}^f = 1/10$ to calculate $\delta_{y,i}^f = 10\delta_{c,i}^f$ and, then, $\alpha_1 = 0.22$ and $\alpha_y = Q_{y,i}^f / \delta_{y,i}^f = 0.3$. In this paper, $\delta_{y,i}^f$ comes from the equal energy criterion between the original pushover curve and its trilinear idealization, which gives the trilinear curves shown in Fig. (4b).

3.1.2. Equivalent SDOF System of the RC Frame

The SDOF system, equivalent to the RC frame, is defined in the hypothesis that all the stories have the same yield displacement, calculated using the mean value, as follows:

$$\delta_y^f = \frac{\sum_{i=1}^n \delta_{yi}^f}{N} \quad (1)$$

where N is the number of stories of the building. Likewise, the same maximum inter-story displacement and corresponding ductility ratio are considered for all the stories, as follows:

$$\delta_i^f = \delta^f \quad (2)$$

$$\mu_i^f = \frac{\delta_i^f}{\delta_y^f} = \frac{\delta^f}{\delta_y^f} = \mu^f \quad (3)$$

Under the aforementioned hypothesis, the pushover curves are idealized using a simplified trilinear model (Fig. 4c). The equivalent height (H_{eq}), mass (M_{eq}), and period (T_μ^f) of the SDOF system, equivalent to the RC frame, are defined as follows:

$$H_{eq} = \frac{\sum_{i=1}^N (m_i \cdot u_i \cdot H_i)}{\sum_{i=1}^N (m_i \cdot u_i)} \quad (4)$$

$$M_{eq} = \frac{(\sum_{i=1}^N m_i \cdot u_i)^2}{\sum_{i=1}^N (m_i \cdot u_i)} \quad (5)$$

$$T_\mu^f = \sqrt{\frac{\mu^f}{\alpha_y}} T^f \quad (6)$$

where m_i is the i -th story mass, u_i is the first mode displacement of the building without dampers at height H_i , while T^f is the fundamental vibration period of the bare frame building. The drift angle of the SDOF frame model is given by:

$$\theta^f = \frac{u_0}{H_{eq}} \quad (7)$$

where u_0 is the displacement of the building MDOF model at the equivalent height H_{eq} . The displacement demand and the corresponding drift angle demand may be calculated from the fundamental vibration period of the equivalent SDOF system, as follows:

$$\theta^f = \frac{S_D(T_\mu^f; \xi_0^f)}{H_{eq}} \cong S_A(T_\mu^f; \xi_0^f) \left(\frac{T_f}{2\pi} \right)^2 \quad (8)$$

where $S_D(T_\mu^f; \xi_0^f)$ and $S_A(T_\mu^f; \xi_0^f)$ are the values of spectral displacement and acceleration of the SDOF system, equivalent to the RC frame, as a function of the corresponding fundamental vibration period T_μ^f and the equivalent viscous

damping ξ_0^f .

3.1.3. Design of the Damped Braces

The SDOF system, equivalent to the damped braces, is designed to meet the performance criteria based on the prefixed value of the target drift angle θ_{max} . For this purpose, the damper to RC frame stiffness ratio $r_d = K^d / K^f$ is calculated using the following closed-form expression proposed by Kasai et al. [28].

$$r_d = \frac{p \left(\left(\frac{\theta^f}{\theta_{max}} \right)^2 - 1 \right) \left(1 + a \left(\xi_0^f + \frac{1}{\pi} \cdot \frac{\alpha_y + \mu^c - \alpha_y^\lambda (1 + \mu^c)}{\alpha_y + \mu^c} \cdot R \right) \right)}{(1 + a \xi_0^f) \left(\gamma_s + \frac{1}{\mu^d} \right) + \frac{2aR}{\pi \mu^d} \left(1 - \frac{1}{\mu^d} \right)} \quad (9)$$

where μ^f and μ^c are the maximum and cracking ductility ratio of the bare frame, μ^d is the damper ductility ratio, $a=25$, $R=0.6$, $\lambda = 0.5$, and γ_s is the steel frame-damper stiffness ratio ($\gamma_s = 0$ if no elastic steel frame connects the dampers to the structure). The lateral stiffness of the SDOF system, equivalent to the damped braces, is then distributed along with the height according to the following optimal dampers distribution rule [5]:

$$K_{d,i} = \frac{V_i \sum_{i=1}^N (K_{\mu,i}^f H_i^2)}{H_i \sum_{i=1}^N (Q_i H_i)} \left(\frac{1}{\gamma_s + 1/\mu^d} + \frac{\mu^f}{\alpha_y} \cdot r_d \right) - \frac{K_{\mu,i}^f}{\gamma_s + 1/\mu^d} \quad (10)$$

where $K_{d,i}$ and V_i are, respectively, the damper lateral stiffness and the design shear force at the i -th story. This stiffness distribution bases on the following constraints:

- 1) The equivalent viscous damping of the MDOF system is the same as the SDOF system;
- 2) The distributions of the drift angle and the ductility demand of the damped braced frame system are uniform along with the height, although those of the RC frame is non-uniform;
- 3) The distribution of the yield drift angle of the dampers is uniform along with the height.

The overall design strength of the damped braces at the i -th story is calculated from the lateral stiffness $K_{d,i}$ as follows:

$$V_{d,i} = K_{d,i} \frac{\theta_t H_i}{\mu^d} \quad (11)$$

The axial stiffness $K_{DB,i}^j$ and strength $P_{DB,i}^j$ of the j -th damped brace at the i -th floor should satisfy the following equations:

$$\sum_{j=1}^n K_{DB,i}^j \cos^2 \theta_j = K_{d,i} \quad \sum_{j=1}^n P_{DB,i}^j \cos^2 \theta_j = V_{d,i} \quad (12)$$

where θ_j is the inclination angle of the j -th brace, and n is the number of the damped braces. The overall story stiffness of the damped braces given by Eq. (12) is then distributed in-plan to increase the torsional stiffness of the building and minimize the impact on the architectural functionality. The axial stiffness $K_{DB,i}^j$ and the axial strength $P_{DB,i}^j$ are then used to size the brace

and the damper. The axial stiffness of the damper ($K_{D,i}^j$) and the axial stiffness of the brace ($K_{B,i}^j$) should satisfy the following equation:

$$K_{DB,i}^j = \frac{1}{\frac{1}{K_{D,i}^j} + \frac{1}{K_{B,i}^j}} \quad (13)$$

Moreover, the axial strength $P_{DB,i}^j$ of the damped brace (i.e., the axial strength of the damper) should be lower than the buckling strength of the brace according to the capacity design rule.

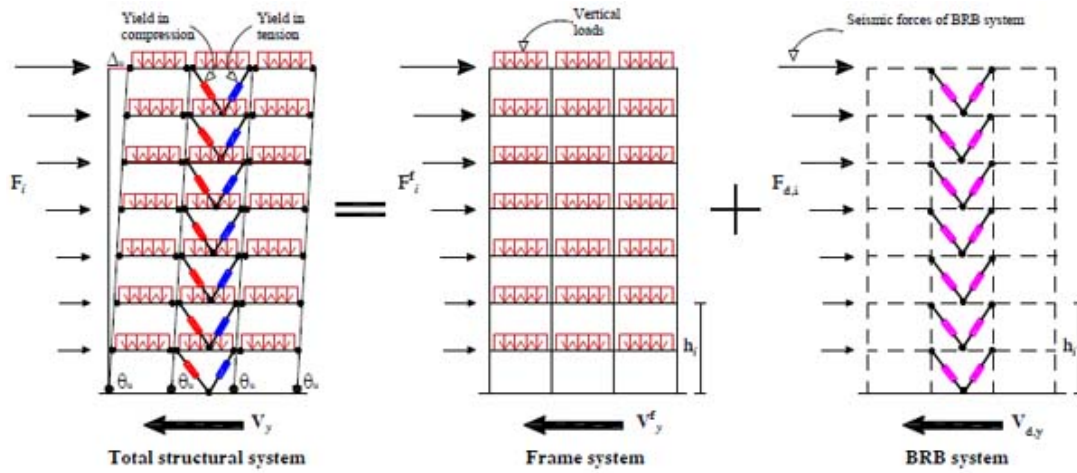


Fig. (1). Decomposition of the structural system into two subsystems.

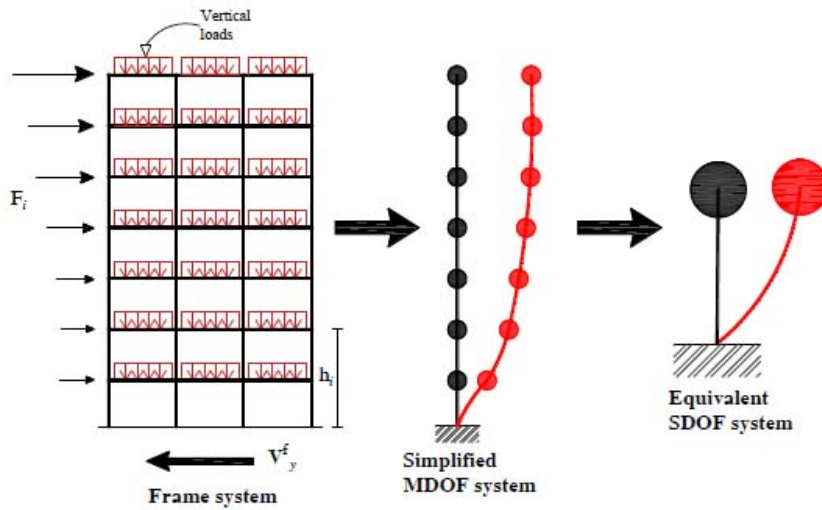


Fig. (2). a) Frame system; b) Simplified MDOF model; c) Equivalent SDOF system.

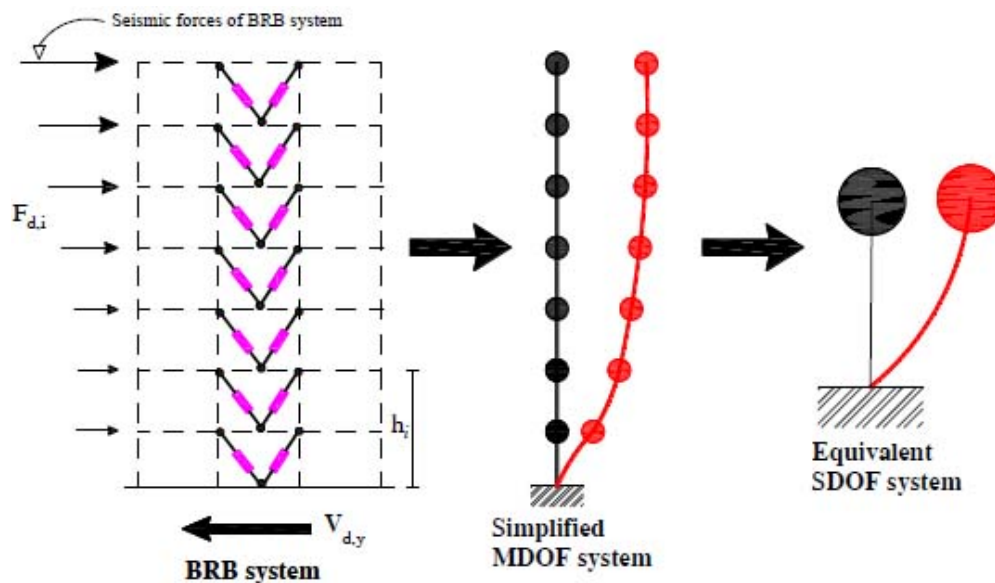


Fig. (3). a) Damped brace system; b) Simplified MDOF model; c) Equivalent SDOF system.

4. RESULTS AND DISCUSSION

4.1. The Case Study RC School Residential Building

4.1.1. Description, in situ Measurements and Laboratory Tests

The case study deals with an eight-story school residential building in Pisa, Tuscany (Italy) Fig. (6). The structure, built at the end of the 1950s, consists of reinforced concrete frames running especially in one direction Figs. (7, 8). The building has a rectangular-shaped floor plan for the first two levels with dimensions of about 23.7x37.5m (Figs. 7, 8), while the other floors have an L-shaped plan (Figs. 9-11). The floors have a mixed structure made up of reinforced concrete and tiles. The following investigations were carried out: 1) geometrical measurements; 2) sub-soil investigations; 3) materials testing on samples taken out from the structure. The sub-soil class, according to Eurocode 8 [12] and Italian Seismic Code [48], was ground type D. The topographic coefficient $S_T = 1.0$ for slope category T_I was considered in the analysis. A nominal life $V_N=50$ years and a class of use III ($C_u=1.5$) were selected, resulting in a reference life $V_R=75$ years. The parameters of the elastic design response spectra used for seismic assessment are plotted in Table 1. The geometry and structural details were known from original outline construction drawings integrated by a direct visual survey. The mechanical properties of the construction materials were taken from limited in-situ testing. Results gave mean values of strength $f_{cm}=27.5$ MPa for concrete and $f_{ym}=378$ MPa for steel rebars. The mean strength values should be divided by the Confidence Factor CF corresponding to the knowledge level. In the case study, due to

the extensive measuring and testing, the full knowledge level KL3 [12, 49] it attained, which implies a Confidence Factor CF = 1.

4.1.2. Seismic Assessment

The seismic performance evaluation was developed according to the Italian Code [48, 49] and Annex B of EN 1998-3 [50].

The Limit States of Immediate Occupancy (IO), Damage Limitation (DL), and Life Safety (LS) were considered in the analysis. The RC framed structure was modeled in SAP2000 [51] finite element computer program (Fig. 12). Fig. (13) shows the first three mode shapes of the existing structure and the corresponding dynamic properties (*i.e.*, period T_i , and modal mass ratios $\alpha_{i,x}$ and $\alpha_{i,y}$ in X- and Y-directions, respectively). A fiber plastic hinge model was implemented for the non-linear analysis.

The concrete was modeled with the stress-strain relationship originally proposed by Mander *et al.* [52]. The steel was modeled with an elastic-plastic-hardening relationship. Two vertical distributions of the lateral loads were applied: a “modal” pattern and a “uniform” pattern distribution. The “modal” pattern (Group 1) is proportional to the lateral forces consistent with the lateral force distribution in the direction under consideration determined in the elastic analysis. The “uniform” pattern (Group 2) uses lateral forces that are proportional to mass. According to Eurocode 8 [12] and Italian Code [48] provisions, the analysis considers an accidental eccentricity of 5% of the building dimension perpendicular to the direction of excitation. The seismic performance evaluation applies the procedure reported in both the Annex B of EN 1998-3 [50] and the current Italian Code [48, 49].

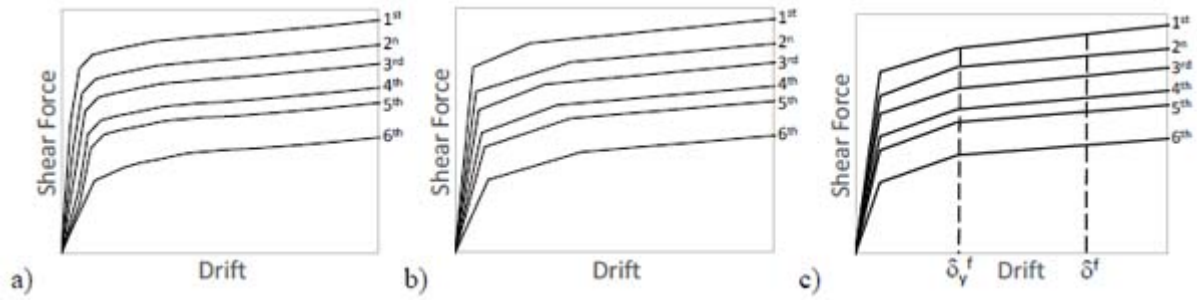


Fig. (4). a) Pushover curves; b) Trilinear idealization; c) Simplified trilinear behavior.

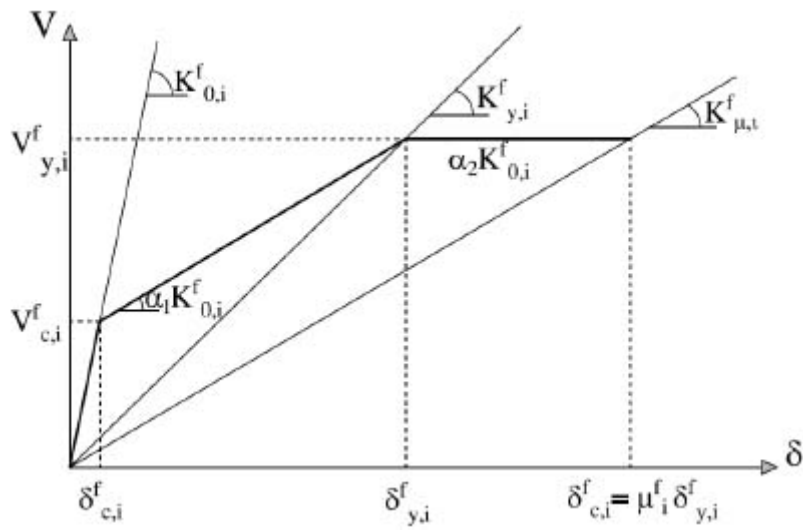


Fig. (5). Trilinear idealization of the pushover curve (*i*-th story shear force vs *i*-th inter-story drift).



Fig. (6). External front view of the building.

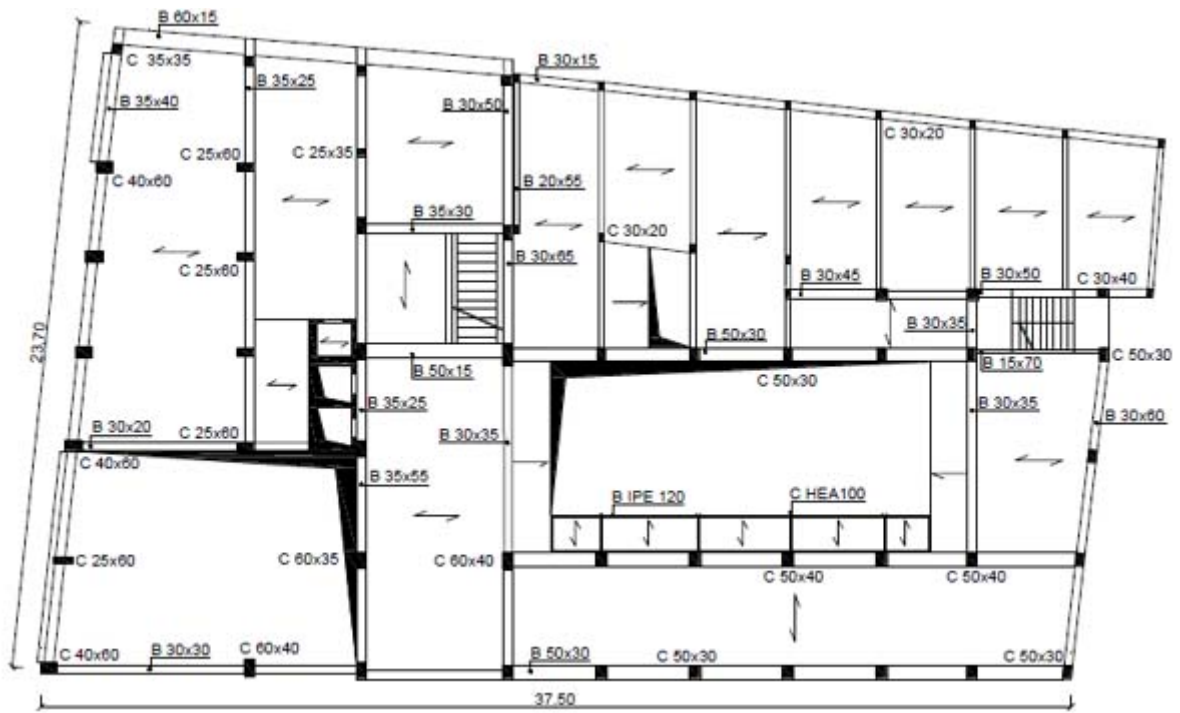


Fig. (7). Plan view of 1st floor.

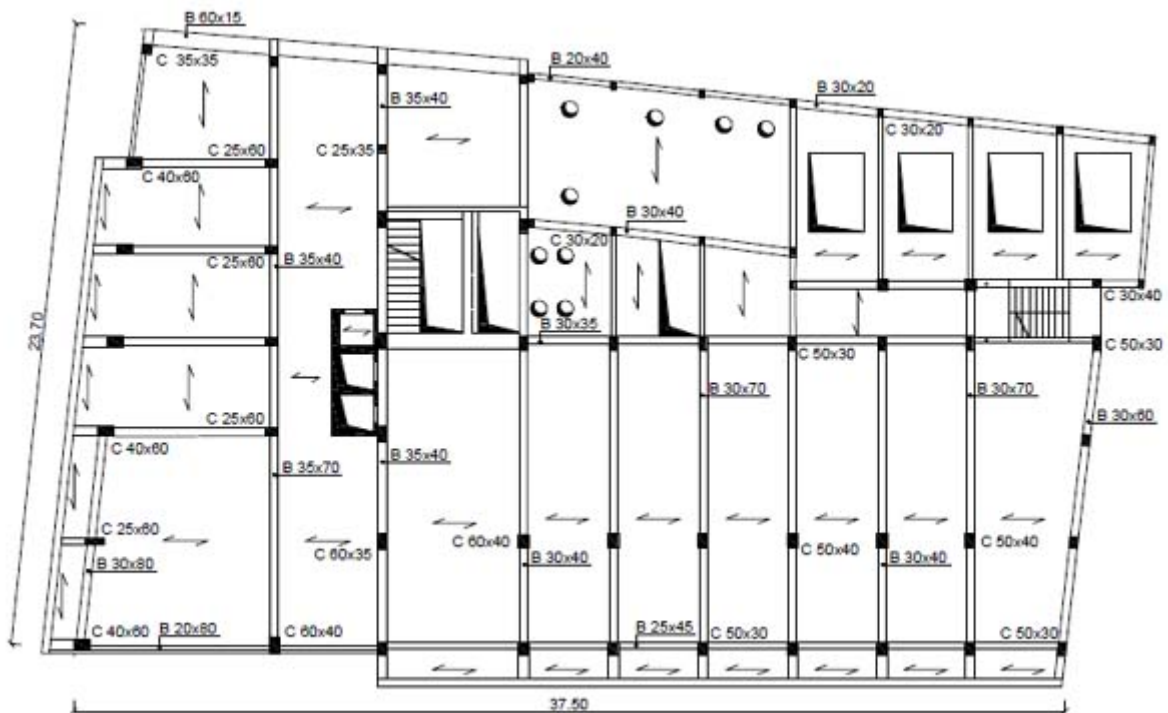


Fig. (8). Plan view of 2nd floor.

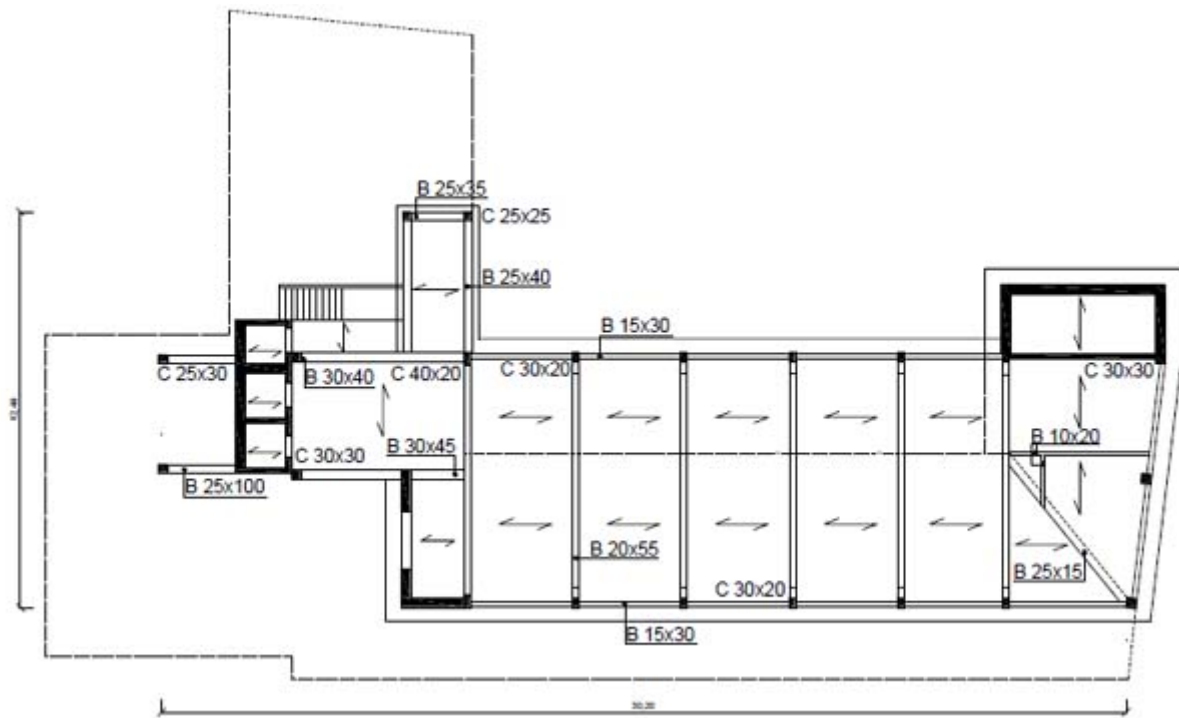


Fig. (11). Plan view of 8th floor.

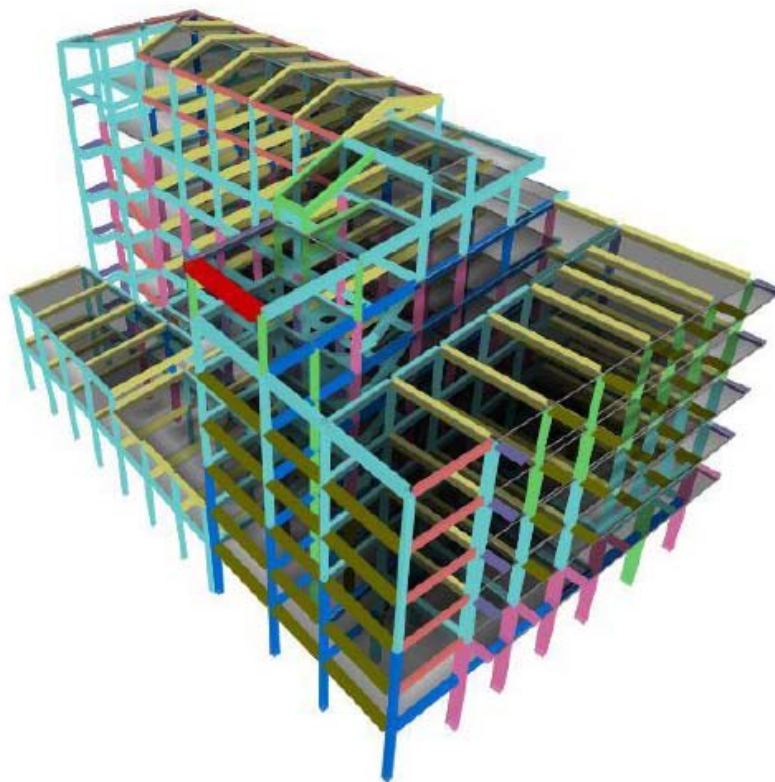


Fig. (12). 3D model of the building.

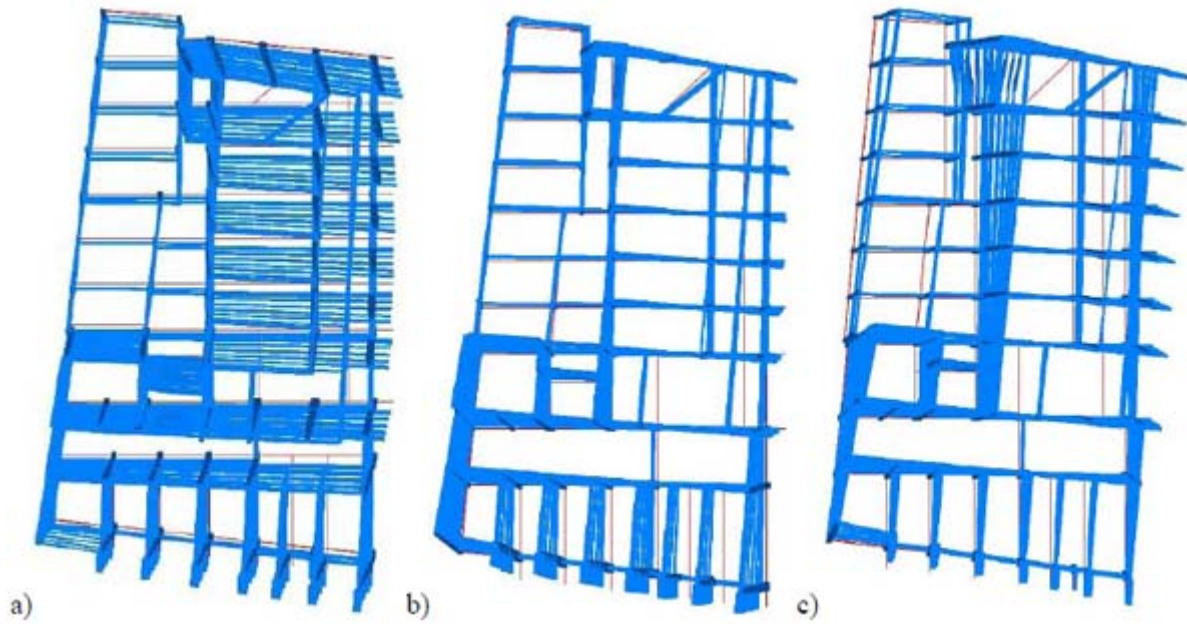


Fig. (13). First three mode shapes of the existing building. **a)** First mode ($T_1=1.22$ s; $\alpha_{1,x}=73.1\%$; $\alpha_{1,y}=0.36\%$) ; **b)** Second mode ($T_2=1.02$ s; $\alpha_{2,x}=6.0\%$; $\alpha_{2,y}=17.1\%$). **c)** Third mode ($T_3=0.968$ s; $\alpha_{3,x}=0.41\%$; $\alpha_{3,y}=67.8\%$).

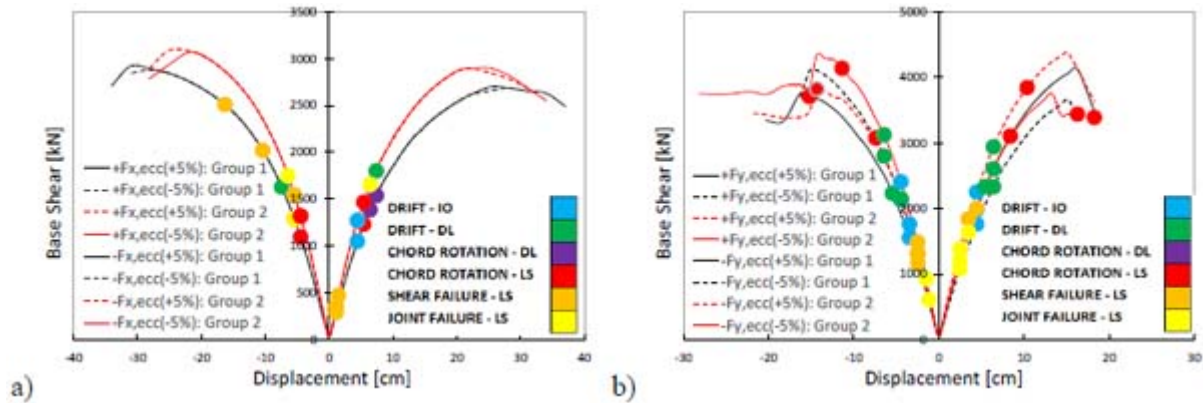


Fig. (14). Pushover curves of the existing building and corresponding limit states. **a)** X-direction; **b)** Y-direction.

The Limit State (LS) of Life Safety (LS) occurs when the seismic demand reaches the structural capacity. The capacity of ductile and brittle members was estimated in terms of chord rotation and shear strength, respectively. The deformation capacity of beams and columns was defined in terms of the chord rotation according to Appendix A of EN 1998-3 [50]. The chord rotation relative to the LS of LS was assumed as 3/4 of the ultimate value given by the formula A.1 of EN 1998-3 [50]. The pushover curves of the existing building and the performance points corresponding to the different limit states are plotted in Fig. (14). The results in X-direction show that the chord rotation limit state of Life Safety (LS) is reached on the linear branch of the pushover curve. The reason for this behavior was the low ductility capacity of the first-story columns of the staircase structure on the right side of the plan (Fig. 7). The poor ductile performance of these columns comes

from their non-seismic reinforcement detailing and high axial force under seismic loading due to the staircase knee beams. Table 2 shows the synthesis of seismic safety verification. The results refer to the following limit states: **a)** Shear failure of RC members, **b)** Beam-column joint failure, **c)** Chord rotation for the LS of Damage Limitation (DL), **d)** Chord rotation for the LS of Life Safety (LS), **e)** Immediate Occupancy (IO), **f)** Damage Limitation (DL), **g)** 15% Strength Reduction in beams. The peak ground acceleration (PGA), return period (T), and safety index (ζ_E) for the different limit states are plotted. Many deficiencies were found: 1) poor shear capacity of brittle components ($\zeta_E = 0.056$ for the shear failure of RC members; $\zeta_E = 0.112$ for beam-column joint failure); 2) Inadequate chord rotation capacity for the LS of LS ($\zeta_E = 0.093$); 3) Inadequate lateral stiffness especially in X-direction for both the LS of IO ($\zeta_E = 0.561$) and the LS of DL ($\zeta_E = 0.727$).

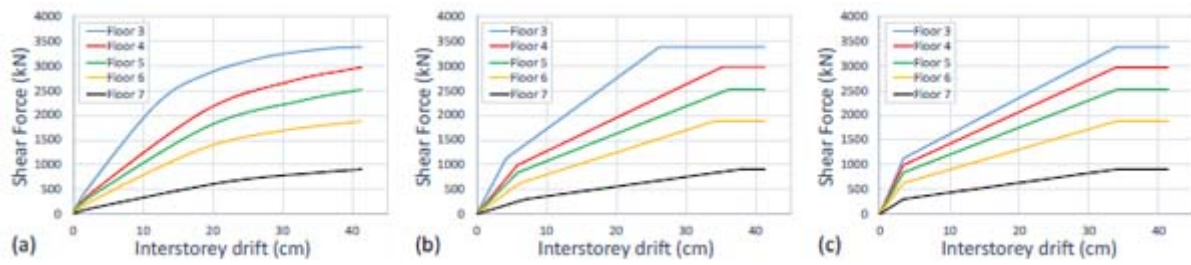


Fig. (15). Pushover analysis in X-Direction. a) Pushover curves; b) Trilinear model; c) Simplified trilinear model.

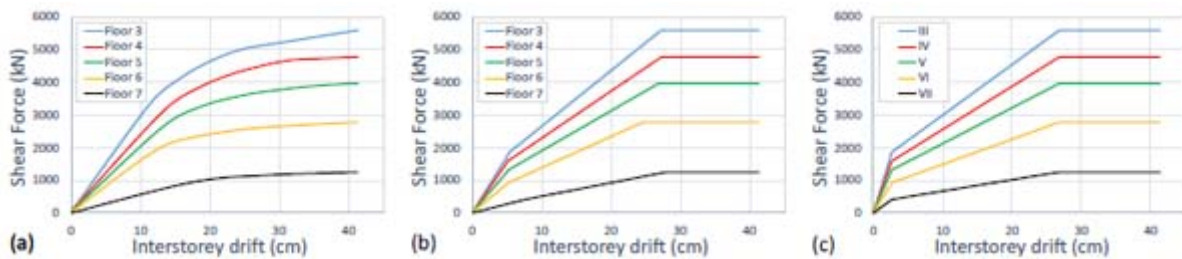


Fig. (16). Pushover analysis in Y-Direction. a) Pushover curves; b) Trilinear model; c) Simplified trilinear model.

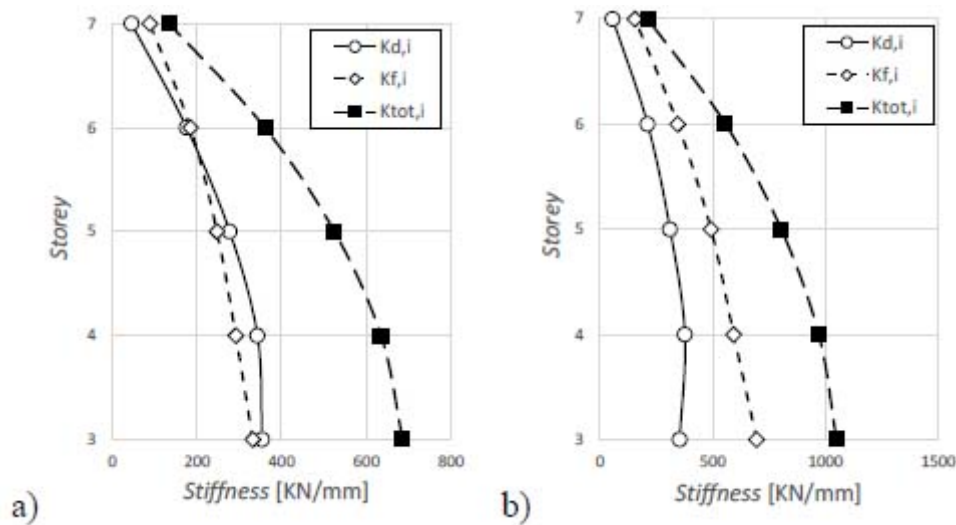


Fig. (17). Optimal damper distribution. (a) X-direction; (b) Y-direction.

4.1.3. Seismic Retrofit with Buckling Restrained Braces

The seismic design of the damped braces was carried out as described in Section 3 above. At first, a pushover analysis was carried out using the first mode distribution of the lateral forces. This approach accurately estimates the seismic response of low-rise and regular buildings where both torsional and higher modes effects are negligible. On the contrary, the existing pre-seismic code buildings are often irregular in plan and/or elevation. Thus, the higher mode effects in plan (torsion) and elevation may strongly influence their seismic response. However, in the case study, the first mode is

dominant in both X- and Y- directions. Moreover, the non-linear static analysis does not highlight a local or soft story mechanism. Figs. (15a-16a) show the pushover curves in X- and Y- directions, respectively. In the case study, the design strategy bases on two global retrofit methods: 1) RC shear walls in the first two stories; 2) buckling restrained braces in the subsequent stories. Moreover, the attic floor is not considered in the design procedure. Thus, Figs. (15-16) show the story pushover curves from 3rd to 7th floor. The trilinear idealization of the pushover curves is shown in Figs. (15b - 16b). The corresponding parameters are plotted in Tables 3 and 4.

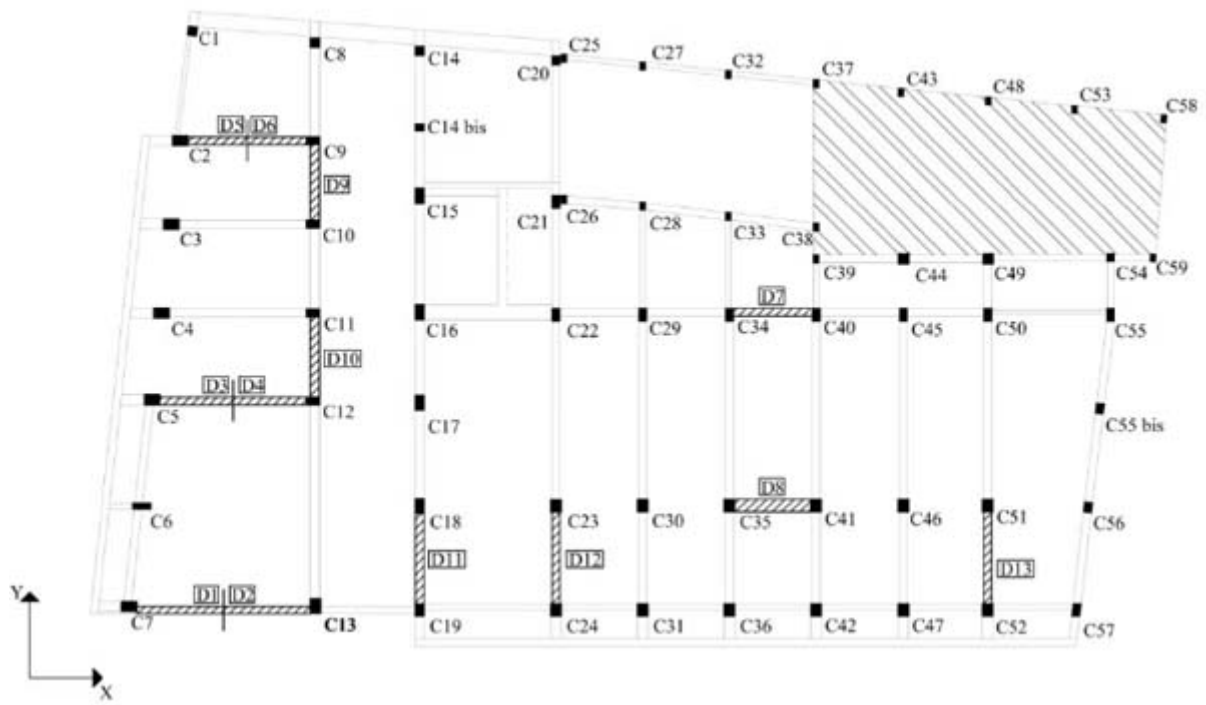


Fig. (18). Location in plan of the damped braces.



Fig. (19). 3D model of the building retrofitted using RC walls and damped braces.

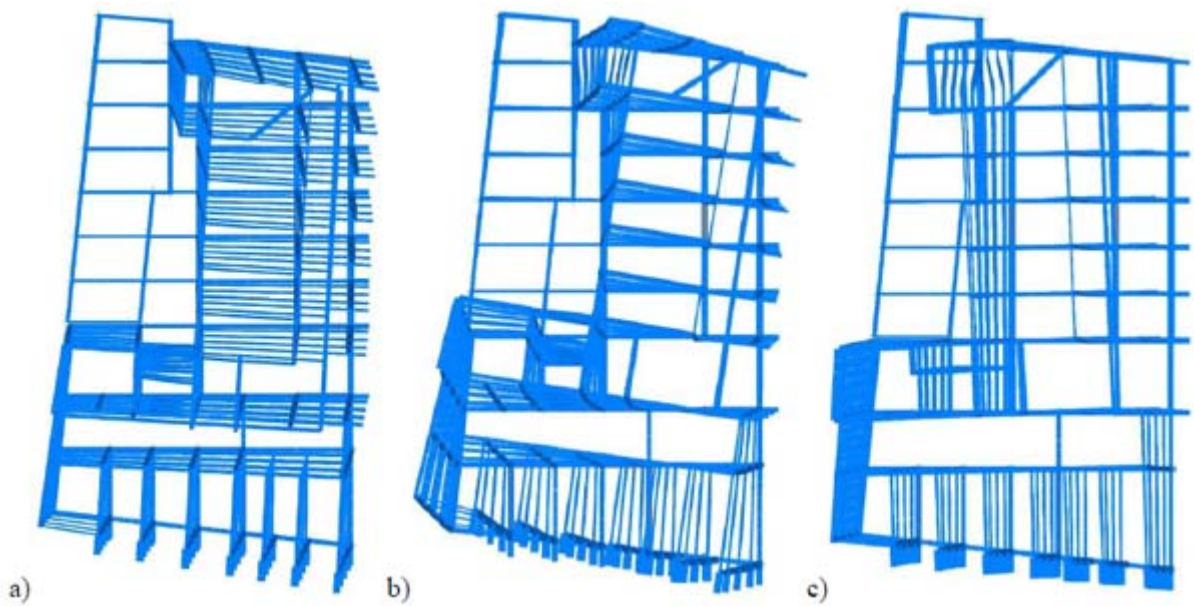


Fig. (20). Fundamental mode shapes of the building retrofitted with damped braces.

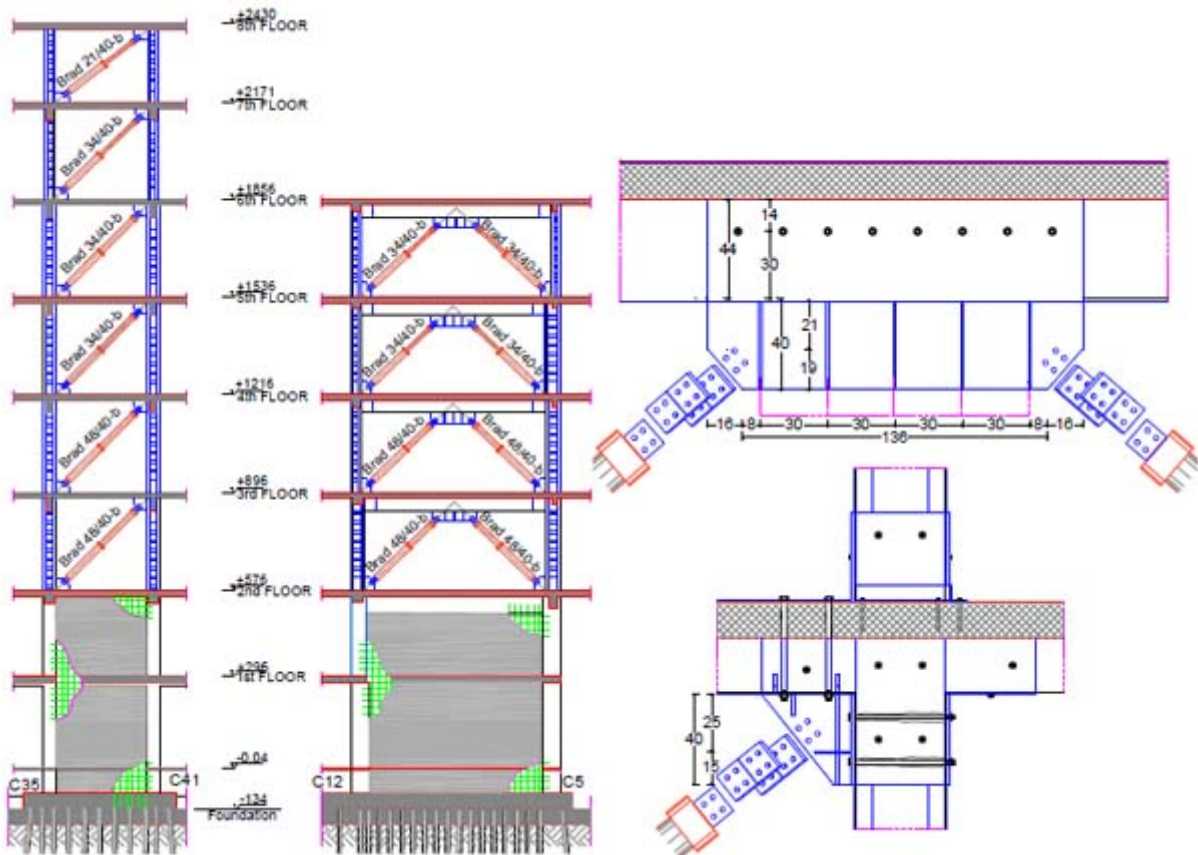


Fig. (21). Section view of the school residential building after retrofitting with damped braces.

The simplified trilinear curves as defined in Section 3.1.1 are plotted in Figs. (15c-16c). In general, both yield and maximum displacement may considerably change from one

story to another, especially for existing pre-seismic code buildings that often exhibit soft-story or torsional failure mechanisms. In this case, the trilinear modeling of the

pushover curves becomes prohibitive. However, this situation does not occur in the case study. The SDOF system, equivalent to the RC frame, was defined based on Eqs. (4-6). The equivalent height H_{eq} and mass M_{eq} are shown in Table 5. The SDOF system, equivalent to the damped braces, was designed using Eq. (9) and considering BRBs with a ductility ratio of 10 and hardening stiffness ratio of 2%. The design parameters are shown in Table 6. The period of the SDOF system, equivalent to the RC frame, assumes different values in X- and Y-directions. Thus, according to Eq. (9) also the damper to frame stiffness ratio r_d has different values in the two directions (*i.e.*, $r_d=1.04$ in X-direction, and $r_d=0.57$ in Y-direction). The lateral stiffness of the SDOF system, equivalent to the damped braces, is then distributed along with the height according to the optimal distribution rule of Eq. (10) (Fig. 17). The in-plan stiffness distribution of the damped braces is then selected to minimize the impact of bracing on architectural functionality and increase the torsional stiffness of the building (Fig. 18). This gives the axial stiffness $K'_{DB,i}$ of each damped brace (Tables 7 and 8) that is used to size the brace and the damper. The values of their stiffness should satisfy Eq. (13). Moreover, according to the hierarchy design criterion, the axial strength $P'_{DB,i}$ of the damped brace (*i.e.*, the axial strength of the damper) should be lower than the buckling strength of the brace. The dampers and braces used in X- and Y-directions are summarized in Tables 9 and 10, respectively. The 3D model of the RC building after retrofit is shown in Fig. (19). The corresponding mode shapes and dynamic properties are plotted in Fig. (20) and Table 11. Finally, it should be highlighted that the retrofit scheme consists of both global (*i.e.*, RC shear walls for the first two stories, and BRBs otherwise) and local retrofit strategies (Fig. 21), including strengthening of columns next to the steel braces by steel angles and strips, shear strengthening of unconfined joints with Fiber-Reinforced Polymers (FRP), shear and bending reinforcement of some beams with FRP and foundation retrofit with micro piles.

4.2. Seismic Assessment of Retrofitted Structure

The effectiveness of the seismic retrofit method is finally demonstrated by the non-linear time-history analysis using the well-known Bouc-Wen model [53] for the hysteretic dampers and the non-linear fiber hinge model for the RC members. The building was subjected to bi-directional excitations representing the two horizontal components of the earthquake ground motion. Following the provisions of the Italian Code [48], two suites of seven earthquake ground motions were selected, the first for the Life Safety (LS) Limit State and the second for the Collapse Prevention (CP) Limit State. The design value of the seismic effect is the average of the response quantities from all the analyses. The SIMBAD database (Selected Input Motions for displacement-based Assessment and Design), the European Strong-motion Database (ESD), and the Italian Accelerometric archive (ITACA) [54, 55] have given the selected accelerograms. Spectrum-compatible signals were obtained scaling real records and observing the following rules provided by the Italian Code [48]: 1) the mean of the zero period spectral response acceleration values is not smaller than $a_g S$, where S is the soil factor and a_g is the design ground acceleration on type A ground; 2) in the range of periods of interest no value of the mean elastic spectrum is less than 90% of the corresponding value of the target elastic spectrum. The parameters of the accelerograms used in the dynamic analysis are plotted in Tables 12 and 13. Their spectrum compatibility and Scaling Factors (SF) are shown in Figs. (22 and 23). The Collapse Prevention (CP) limit state was verified by direct comparison of the calculated displacement ductility demand of the hysteretic dampers to the corresponding displacement ductility capacity. Figs. (24 and 25) show the hysteresis loops of some dampers in X- and Y-direction, respectively, under the seven time-histories considered for the Collapse Prevention Limit State.

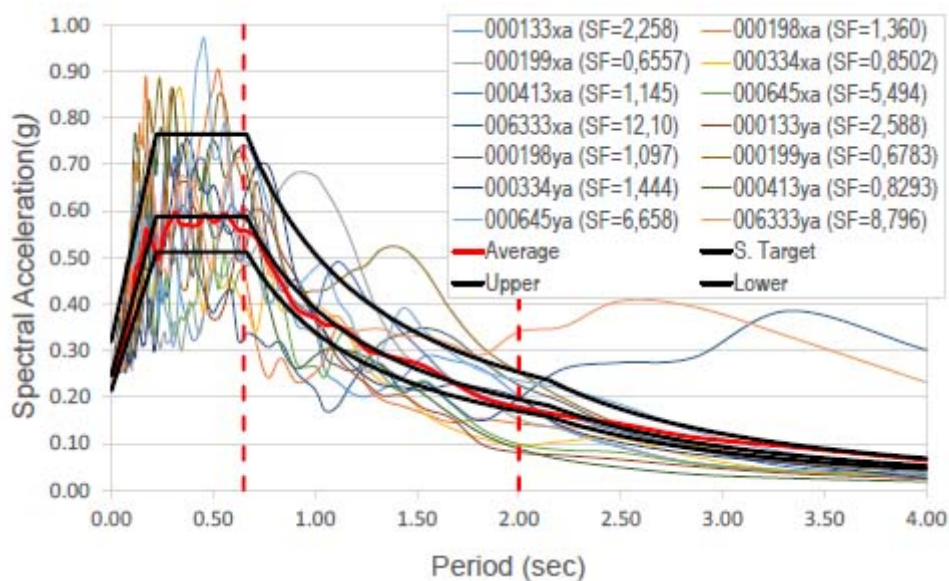


Fig. (22). Spectrum compatibility of selected records for LS Limit State.

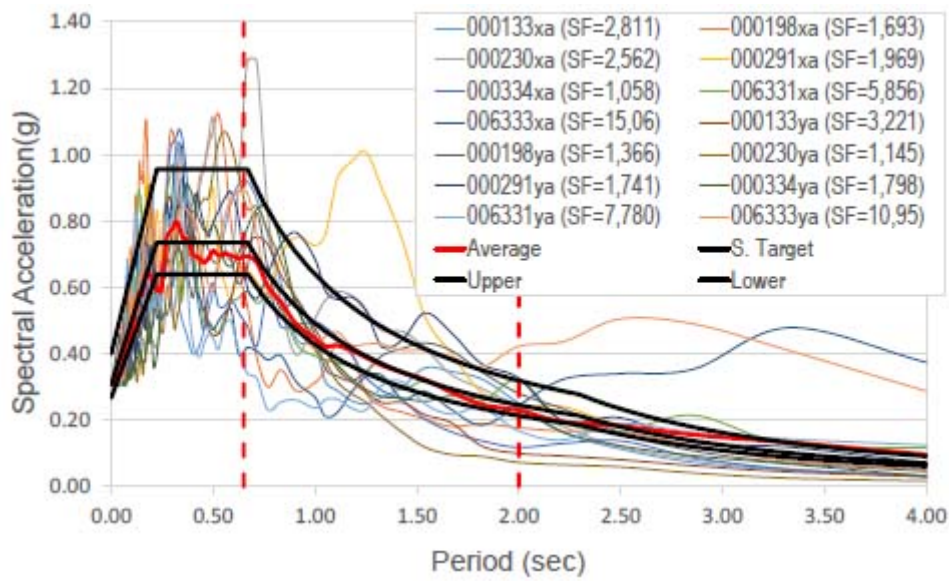


Fig. (23). Spectrum compatibility of selected records for CP Limit State.

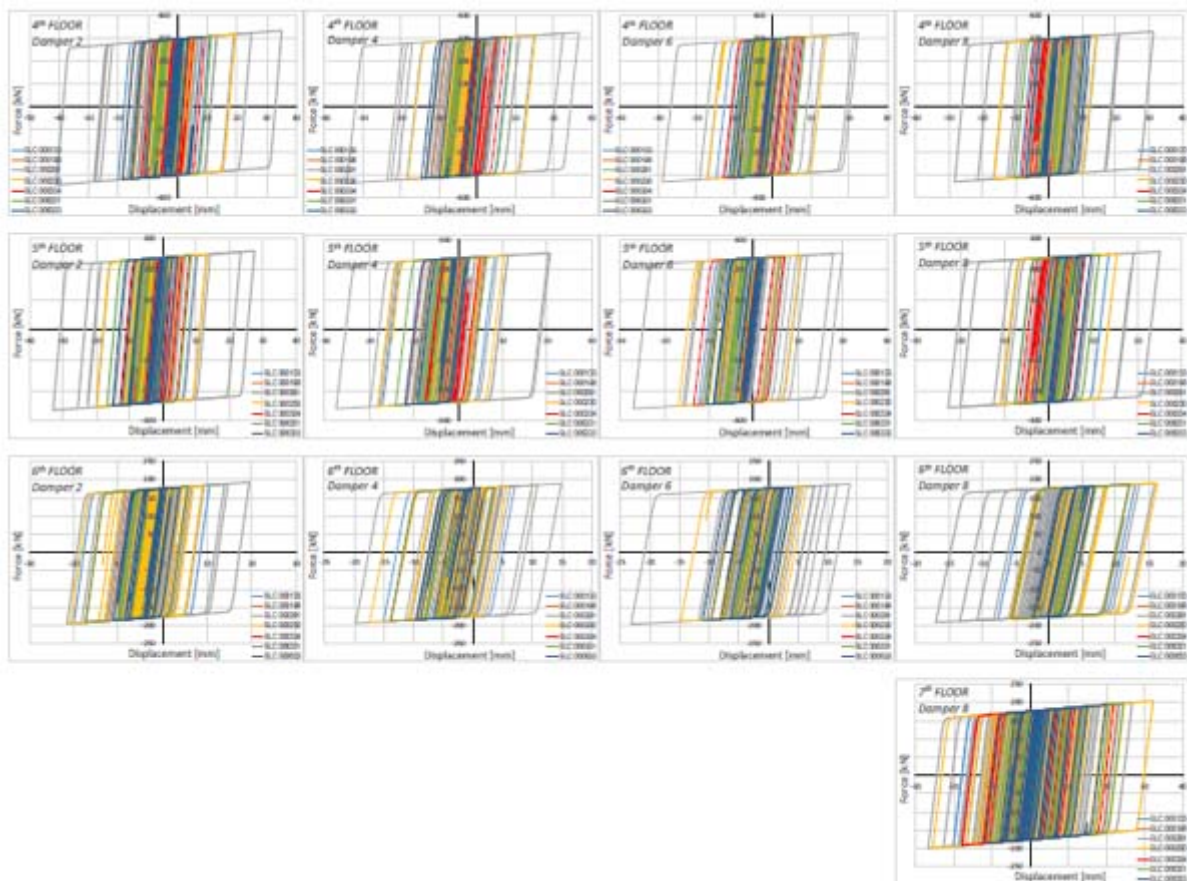


Fig. (24). Hysteresis loop of some dampers in X-Direction. Collapse Prevention Limit State.

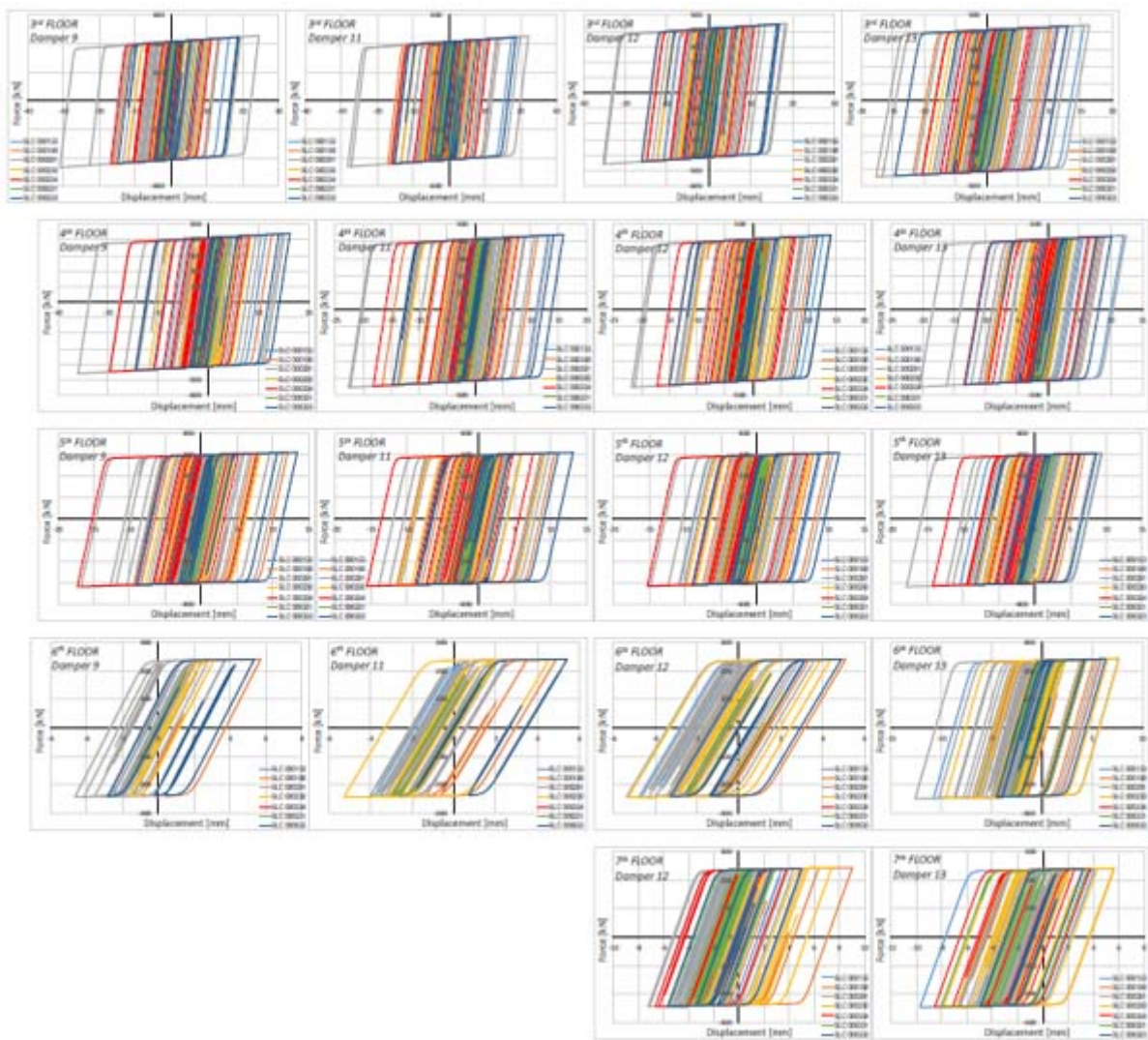


Fig. (25). Hysteresis loops of some dampers in Y-Direction. Collapse Prevention Limit State.

Very large plastic strains were observed in all the dampers, thus evidencing the effectiveness of the design method. The average of the peak displacements from the seven earthquakes was used as the design value of the seismic effect. It should be highlighted that no damper exceeds its capacity of 20 mm, corresponding to its displacement ductility capacity ratio $\mu^d=10$. According to both Eurocode 8 [12] and Italian Code [48, 49], the Life Safety verification compared the member chord rotation demand in beams and columns to the corresponding chord rotation capacity. As far as columns are concerned, this comparison is carried out in terms of inter-story drift. The demand is given by the inter-story drift time-histories for the selected earthquake records. The capacity is represented by the limit domain for the limit states of Life Safety (LS) and Damage Limitation (DL) calculated from the corresponding chord rotation. For the Limit State of Damage Limitation (DL),

the chord rotation at yielding (θ_y) was estimated by the formula (A.10b) and (A.11b) from EN 1998-3 [50]. For the Limit State of Life Safety (LS), the chord rotation is assumed as 3/4 of the ultimate chord rotation θ_u defined by the formula A.1 from EN 1998-3 [50]. In columns, under seismic ground motion, the nodal rotation is low compared to the drift Δ of the equivalent cantilever. Thus, the chord rotation θ is given by Δ/L_s , where L_s is the shear span length considered placed at the middle of the column. The drift capacity depends on the direction of the bending axle in bi-axial bending. However, a study available in the literature [56] shows that the interaction diagram is circular if the components of chord rotation along the sides of the section in bi-axial bending are normalized to the corresponding chord rotations in uniaxial loading. Fig. (26) shows the comparison between capacity and demand in terms of the maximum inter-story drift of the columns.

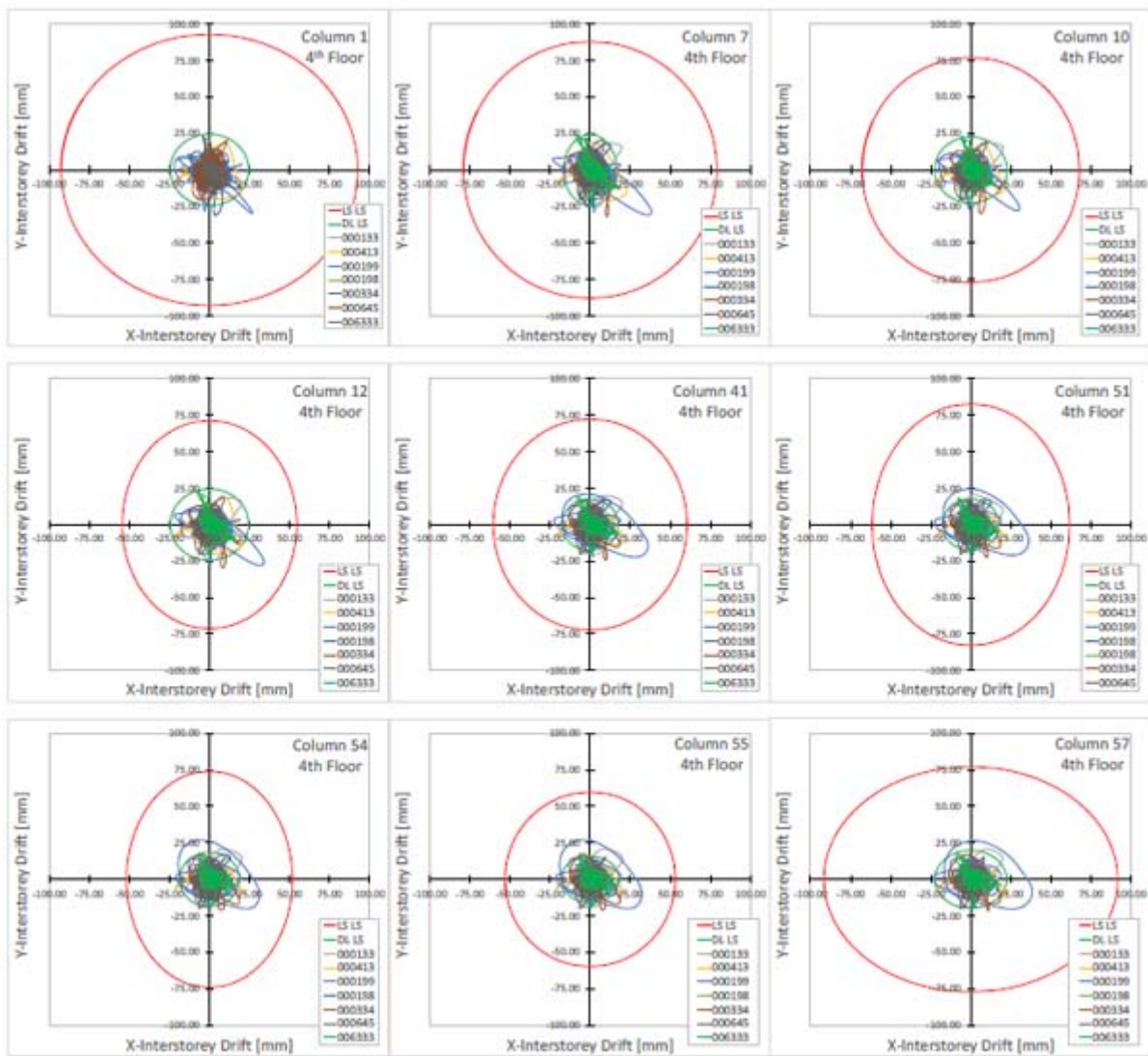


Fig. (26). Drift time-histories and limit domains in some columns. Collapse Prevention Limit State.

Table 1. Parameters of elastic design response spectra.

Limit State	IO	DL	LS	CP
Probability of exceedance P_{VR}	0.81	0.63	0.10	0.05
Return Period T_R (years)	45	75	712	1462
Peak ground acceleration PGA/g	0.046	0.056	0.137	0.173
Amplification factor F_o	2.553	2.567	2.391	2.385
Transition Period T_C (s)	0.243	0.259	0.281	0.286

Table 2. Limit states and corresponding PGA, Return Period (T) and safety index (ζ_E).

Limit State	Comb.	Group	PGA [g]	T [years]	ζ_E
a) Shear failure of RC members	- F_y , ecc(-5%)	1	0.00786	6	0.056
b) Beam-column joint failure	- F_x , ecc(+5%)	1	0.0157	12	0.112
c) Chord Rotation DL	- F_y , ecc(-5%)	2	0.0337	26	0.797

Limit State	Comb.	Group	PGA [g]	T [years]	ζ_E
d) Chord Rotation LS	-F _y + ecc(+5%)	1	0.0129	10	0.093
e) Drift IO	-F _y , ecc(-5%)	1	0.0258	20	0.561
f) Drift DL	-F _y , ecc(-5%)	2	0.0410	34	0.727
g) 15% Strength Reduction in beams	+F _y , ecc(-5%)	1	0.1730	1455	1.252

Table 3. Parameters of trilinear idealization of pushover curves in X-Direction.

Floor	δ'_{ci} [mm]	Q'_{ci} [kN]	δ'_{yi} [mm]	Q'_{yi} [kN]	K'_{oi} [kN/mm]	$\alpha_i K'_{oi}$ [kN/mm]	δ'_i [mm]	μ'_i	K'_{yi} [kN/mm]	$K'_{\mu i}$ [kN/mm]
3	3.39	1126.56	33.92	3379.67	332.11	73.80	41.33	1.22	99.63	81.77
4	3.39	990.59	33.92	2971.76	292.02	64.89	41.33	1.22	87.61	71.90
5	3.39	839.65	33.92	2518.96	247.53	55.01	41.33	1.22	74.26	60.94
6	3.39	626.72	33.92	1880.17	184.76	41.06	41.33	1.22	55.43	45.49
7	3.39	301.98	33.92	905.95	89.02	19.78	41.33	1.22	26.71	21.92

Table 4. Parameters of trilinear idealization of pushover curves in Y-Direction.

Floor	δ'_{ci} [mm]	Q'_{ci} [kN]	δ'_{yi} [mm]	Q'_{yi} [kN]	K'_{oi} [kN/mm]	$\alpha_i K'_{oi}$ [kN/mm]	δ'_i [mm]	μ'_i	K'_{yi} [kN/mm]	$K'_{\mu i}$ [kN/mm]
3	2.68	1863.94	26.81	5591.83	695.13	154.47	41.33	1.54	208.54	135.29
4	2.68	1590.59	26.81	4771.78	539.19	131.82	41.33	1.54	177.96	115.45
5	2.68	1321.49	26.81	3964.46	492.83	109.52	41.33	1.54	147.85	95.91
6	2.68	926.21	26.81	2778.64	345.42	76.76	41.33	1.54	103.63	67.23
7	2.68	418.00	26.81	1254.00	155.89	34.64	41.33	1.54	46.77	30.34

Table 5. Story masses and heights ($H_{eq} = 10.59$ m; $M_{eq} = 1648.75$ kNs²/m).

Floor	m_i [kNs ² /m]	H_i [m]	$m_i \times H_i^2$ [kNs ² m]	$m_i \times H_i$ [kNs ²]
3	450.75	3.1	4333.71	1397.33
4	443.18	6.2	17035.66	2747.69
5	438.81	9.3	37952.45	4080.91
6	456.62	12.4	70209.23	5662.03
7	230.42	15.5	55357.91	3571.48
-	-	-	184886.95	17459.43

Table 6. Design parameters of SDOF model of dampers.

Direction	a	R	λ	γ_s	p	α_y	T_f [s]	T_μ^f [s]	S_D [m]	θ_f	θ_{max}	ζ^d	μ^d	r_d
X	25	0.60	0,50	0.05	0.25	0.30	1.02	2.06	0.25	0.0237	0.0133	0.03	7.00	1.04
Y	25	0.60	0,50	0.05	0.19	0.30	0.754	1.71	0.21	0.0197	0.0130	0.03	8.00	0.57

Table 7. Design lateral stiffness and strength of damped braces in X-Direction.

Floor	Q_i [kN]	$K'_{\mu i}$ [kN/mm]	$K_{d,i}$ [kN/mm]	n	$K_{d,i}/n$ [kN/mm]	Dampers 1-2		Dampers 3-4		Dampers 5-6		Damper 7		Damper 8	
						$K_{DB,i}$ [kN/mm]	θ [°]	$K_{DB,i}$ [kN/mm]	θ [°]	$K_{DB,i}$ [kN/mm]	θ [°]	$K_{DB,i}$ [kN/mm]	θ [°]	$K_{DB,i}$ [kN/mm]	θ [°]
3	14938	81.77	354.26	8	44.28	58.03	40.26	61.60	44.04	68.29	49.58	59.93	42.36	59.93	42.36
4	13742	71.90	343.15	8	42.89	56.21	40.26	59.67	44.04	66.15	49.58	58.05	42.36	58.05	42.36
5	11391	60.94	277.48	8	34.68	45.45	40.26	48.25	44.04	53.49	49.58	46.94	42.36	46.94	42.36

Floor	Q_i [kN]	$K'_{\mu,i}$ [kN/mm]	$K_{d,i}$ [kN/mm]	n	$K_{d,i}/n$ [kN/mm]	Dampers 1-2		Dampers 3-4		Dampers 5-6		Damper 7		Damper 8	
						$K_{DB,i}$ [kN/mm]	θ [°]	$K_{DB,i}$ [kN/mm]	θ [°]	$K_{DB,i}$ [kN/mm]	θ [°]	$K_{DB,i}$ [kN/mm]	θ [°]	$K_{DB,i}$ [kN/mm]	θ [°]
6	7899.98	45.49	175.71	8	21.96	28.78	40.26	30.55	44.04	33.87	49.58	29.72	42.36	29.72	42.36
7	3055.67	21.92	45.54	2	22.97	29.84	40.26	31.68	44.04	35.12	49.58	30.82	42.36	30.82	42.36

Table 8. Design lateral stiffness and strength of damped braces in Y-Direction.

Floor	Q_i [kN]	$K'_{\mu,i}$ [kN/mm]	$K_{d,i}$ [kN/mm]	n	$K_{d,i}/n$ [kN/mm]	Damper 9		Damper 10		Dampers 11-12		Damper 13	
						$K_{DB,i}$ [kN/mm]	θ [°]	$K_{DB,i}$ [kN/mm]	θ [°]	$K_{DB,i}$ [kN/mm]	θ [°]	$K_{DB,i}$ [kN/mm]	θ [°]
3	14938	135.29	354.06	5	70.81	97.46	43.40	95.44	42.10	88.85	37.16	88.85	37.16
4	13742	115.45	377.23	5	75.45	103.84	43.40	101.68	42.10	94.67	37.16	94.67	37.16
5	11391	95.91	311.46	5	62.29	85.74	43.40	83.95	42.10	78.16	37.16	78.16	37.16
6	7900.0	67.23	211.94	5	42.39	58.34	43.40	57.13	42.10	53.19	37.16	53.19	37.16
7	3055.7	30.34	57.20	2	28.60	39.36	43.40	38.54	42.10	35.89	37.16	35.89	37.16

Table 9. Design parameters of dampers and braces in X-Direction.

N.	Damper		Brace 1-2			Brace 3-4			Brace 5-6			Brace 7			Brace 8		
	Type	K_D [kN/mm]	Type	K_B [kN/mm]	L_B [mm]	Type	K_B [kN/mm]	L_B [mm]	Type	K_B [kN/mm]	L_B [mm]	Type	K_B [kN/mm]	L_B [mm]	Type	K_B [kN/mm]	L_B [mm]
3	34-40	153.00	φ114.3/5	113.86	4797	φ114.3/5	127.42	4460	φ114.3/5	147.60	4072	φ114.3/5	121.37	4601	φ114.3/5	121.37	4601
4	34-40	123.00	φ114.3/5	113.86	4797	φ114.3/5	127.42	4460	φ114.3/5	147.60	4072	φ114.3/5	121.37	4601	φ114.3/5	121.37	4601
5	27-40	123.00	φ114.3/4	90.87	4797	φ114.3/4	101.54	4460	φ114.3/4	117.36	4072	φ114.3/4	96.78	4601	φ114.3/4	96.78	4601
6	21-40	88.00	φ101.6/4	80.41	4797	φ101.6/4	89.85	4460	φ101.6/4	103.85	4072	φ101.6/4	85.64	4601	φ101.6/4	85.64	4601
7	21-40	88.00	-	-	-	-	-	-	-	-	-	φ101.6/4	85.64	4601	φ101.6/4	85.64	4601

Table 10. Design parameters of dampers and braces in Y-Direction.

N.	Damper		Brace 9			Brace 10			Brace 11-12			Brace 13		
	Type	K_D [kN/mm]	Type	K_B [kN/mm]	L_B [mm]	Type	K_B [kN/mm]	L_B [mm]	Type	K_B [kN/mm]	L_B [mm]	Type	K_B [kN/mm]	L_B [mm]
3	48-40	210.00	φ168.3/6	223.77	4512	φ168.3/6	215.35	4624	φ168.3/6	184.02	5132	φ168.3/6	184.02	5132
4	48-40	210.00	φ168.3/6	223.77	4512	φ168.3/6	215.35	4624	φ168.3/6	184.02	5132	φ168.3/6	184.02	5132
5	34-40	153.00	φ177.8/5	197.15	4512	φ177.8/5	189.76	4624	φ177.8/5	162.27	5132	φ177.8/5	162.27	5132
6	27-40	123.00	φ114.3/5	123.42	4512	φ114.3/5	118.85	4624	φ114.3/5	101.83	5132	φ114.3/5	101.83	5132
7	27-40	123.00	-	-	-	-	-	-	φ114.3/5	101.83	5132	φ114.3/5	101.83	5132

Table 11. Periods, frequencies, and mass ratios of mode shapes of retrofitted building.

N.	Description	Period (s)	Frequency (Hz)	Modal mass ratio	
				X-Dir.	Y-Dir.
1	Flexural X -Torsional	0.732	1.366	0.43	0.00
2	Torsional	0.677	1.477	0.04	0.12
3	Flexural Y	0.626	1.599	0.00	0.42

Table 12. Suite of earthquake natural records selected for LS Limit State.

Waveform ID	Earthquake Name	Date	M_w	Epicentral Distance [km]	PGA_x	PGA_y
133	Kalamata	13/09/1986	5.9	10	2.1082	2.9095
198	Umbria Marche	14/10/1997	5.6	26	0.4392	0.3624
199	Montenegro	15/04/1979	6.9	16	3.6801	3.5573

Waveform ID	Earthquake Name	Date	M_w	Epicentral Distance [km]	PGA_x	PGA_y
334	Alkion	24/02/1981	6.6	19	2.8382	1.6705
413	Kalamata	13/09/1986	5.9	10	2.1082	2.9095
645	Umbria Marche	14/10/1997	5.6	26	0.4392	0.3624
6333	Montenegro	15/04/1979	6.9	12	1.7743	2.1985

Table 13. Suite of earthquake natural records selected for CP Limit State

Waveform ID	Earthquake Name	Date	M_w	Epicentral Distance [km]	PGA_x	PGA_y
133	Friuli	15/09/1976	6	9	1.069	0.932
198	Montenegro	15/04/1979	6.9	21	1.774	2.199
230	Montenegro	24/05/1979	6.2	8	1.172	2.624
291	Campano Lucano	23/11/1980	6.9	16	1.526	1.725
334	Alkion	24/02/1981	6.6	19	2.838	1.671
6331	South Iceland	21/06/2000	6.4	22	0.513	0.386
6333	South Iceland	21/06/2000	6.4	28	0.199	0.274

The results show that the chord rotation capacity for the LS of DL is exceeded in many cases, while the chord rotation capacity of columns is never exceeded for the LS of LS. Hence, the seismic retrofit using buckling restrained braces proved to be effective in limiting the structural damage related to story drifts and inelastic deformations.

CONCLUSION

The European codes still fail to give any design guidelines for steel dampers. On the other side, both American and Japanese standards propose design procedures that are mostly applied to steel building structures, while the applications to complex real RC buildings are still lacking. This paper presents the retrofit design process of an eight-story reinforced concrete school residential building retrofitted using buckling restrained braces. The design procedure bases on decomposing the dual RC-BRB systems into two subsystems: the RC frame system and the BRB system that is designed to meet the performance criteria based on a target drift angle. The in-plan distribution of damped braces is selected to increase the torsional stiffness of the building while minimizing the impact of bracing on architectural functionality. The vertical distribution of damped braces is finally determined based on an optimal damper distribution rule to attain a uniform distribution of the ductility demand. The following conclusions may be drawn:

- Based on the example building, the design procedure (based on pushover analysis, equivalent SDOF system, and performance-based design using a target drift) shows to be feasible and effective.
- Non-linear response-history analysis results indicate that the complex RC school residential building retrofitted with BRBs responds according to the predictions of the design method.
- The seismic response of the RC building case study, including the maximum inter-story drift ratio and the maximum BRB ductility demand, indicates that the design method achieves the damage-controlled performance objectives.

- The hysteretic loops under different earthquake ground motions show that the optimal damper distribution rule is effective to obtain nearly uniform ductility demand in all the dampers.
- Placing the damped braces is crucial to prevent torsional effects during earthquake ground and keep most areas of the building fully operational during the retrofit implementation.

Therefore, it can be concluded that the proposed retrofit design method was developed and implemented successfully on a complex RC building retrofitted with buckling restrained braces. However, it should be highlighted that the design procedure is based on several simplifying assumptions that, in some cases, can undermine its general validity in the current practice. First, when applying the displacement-based design approach, the SDOF assumption should be checked. In general, normal low-rise buildings can be modeled as an equivalent SDOF system using the pushover method. On the contrary, this assumption may fail for irregular or high-rise RC buildings since it neglects both torsional and higher-mode effects. Moreover, the pushover method applied to the existing building neglects both global and local interaction between the RC frame and the bracing system, thus underestimating the local forces due to bracing. Finally, the same yield and maximum displacements are considered for all the stories, while the existing RC buildings often exhibit soft-story or torsional failure mechanisms. Thus, further research is required to address this knowledge gap.

CONSENT FOR PUBLICATION

Not applicable.

AVAILABILITY OF DATA AND MATERIALS

Not applicable.

FUNDING

None.

CONFLICT OF INTEREST

The authors declare no conflict of interest, financial or otherwise.

ACKNOWLEDGEMENTS

Many thanks to the professional team of "Aires Ingegneria" for the support activities.

REFERENCES

- [1] M. Ferraioli, and A. Mandara, "Base isolation for seismic retrofitting of a multiple building structure: Evaluation of equivalent linearization method", *Math. Probl. Eng.*, vol. 8934196, 2016. [http://dx.doi.org/10.1155/2016/8934196]
- [2] M. Ferraioli, and A. Mandara, "Base isolation for seismic retrofitting of a multiple building structure: Design, construction and assessment", *Math. Probl. Eng.*, vol. 4645834, 2017. [http://dx.doi.org/10.1155/2017/4645834]
- [3] I. Takewaki, *Building control with passive dampers: Optimal Performance-based Design for Earthquakes.*, Wiley, 2009. [http://dx.doi.org/10.1002/9780470824931]
- [4] K. Kasai, Y. Fu, and A. Watanabe, "Passive control systems for seismic damage mitigation", *J. Struct. Eng.*, vol. 124, no. 5, pp. 501-512, 1998. [http://dx.doi.org/10.1061/(ASCE)0733-9445(1998)124:5(501)]
- [5] F. Sutcu, T. Takeuchi, and R. Matsui, "Seismic retrofit design method for RC buildings using buckling-restrained braces and steel frames", *J. Construct. Steel Res.*, vol. 101, pp. 304-313, 2014. [http://dx.doi.org/10.1016/j.jcsr.2014.05.023]
- [6] A. Formisano, C. Castaldo, and G. Chiumiento, "Optimal seismic upgrading of a reinforced concrete school building with metal-based devices using an efficient multi-criteria decision-making method", *Struct. Infrastruct. Eng.*, vol. 13, no. 11, pp. 1373-1389, 2017. [http://dx.doi.org/10.1080/15732479.2016.1268174]
- [7] A. Formisano, L. Lombardi, and F.M. Mazzolani, "Full and perforated metal plate shear walls as bracing systems for seismic upgrading of existing rc buildings", *Ing. Sism.*, vol. 33, no. 1-2, pp. 16-34, 2016.
- [8] G. De Matteis, and M. Ferraioli, "Metal shear panels for seismic upgrading of RC buildings: A case study", *Key Eng. Mater.*, vol. 763, pp. 1058-1066, 2018. www.scientific.net/KEM.763.1058 [http://dx.doi.org/10.4028/www.scientific.net/KEM.763.1058]
- [9] M. Dolce, D. Cardone, and R. Marnetto, "Implementation and testing of passive control devices based on shape memory alloys", *Earthquake Eng. Struct. Dynam.*, vol. 29, pp. 945-968, 2000. [http://dx.doi.org/10.1002/1096-9845(200007)29:7<945::AID-EQE958>3.0.CO;2-#]
- [10] M. Ferraioli, D. Nuzzo, and A. Concilio, "Shape memory alloys for earthquake building protection", *Proceedings of SPIE - The International Society for Optical Engineering*, 2019 [http://dx.doi.org/10.1117/12.2513605]
- [11] *ASCE/SEI 7-05 - American Society of Civil Engineers (ASCE), Minimum design loads for buildings and other structures*, ASCE Standard, 2006.
- [12] *EN 1998-1:2004 - Comité Européen de Normalisation CEN, Eurocode 8 - Design provisions for earthquake resistance of structures*, European Communities for Standardization: Brussels, Belgium, 2004.
- [13] P. Foraboschi, "Bending load-carrying capacity of reinforced concrete beams subjected to premature failure", *Materials (Basel)*, vol. 12, no. 19, p. E3085, 2019. [http://dx.doi.org/10.3390/ma12193085] [PMID: 31546653]
- [14] P. Foraboschi, "Predictive formulation for the ultimate combinations of axial force and bending moment attainable by steel members", *Int. J. Steel Struct.*, vol. 20, no. 2, pp. 705-724, 2020. [http://dx.doi.org/10.1007/s13296-020-00316-6]
- [15] J.L. Bai, and J.P. Ou, "Earthquake-resistant design of buckling-restrained braced RC moment frames using performance-based plastic design method", *Eng. Struct.*, vol. 107, pp. 66-79, 2016. [http://dx.doi.org/10.1016/j.engstruct.2015.10.048]
- [16] F. Barbagallo, M. Bosco, E.M. Marino, P.P. Rossi, and P.R. Stramondo, "A multi-performance design method for seismic upgrading of existing RC frames by BRBs", *Earthquake Eng. Struct. Dynam.*, vol. 46, no. 7, pp. 1099-1119, 2017. [http://dx.doi.org/10.1002/eqe.2846]
- [17] A.V. Bergami, and C. Nuti, "A design procedure of dissipative braces for seismic upgrading structures", *Earthq. Struct.*, vol. 4, no. 1, pp. 85-108, 2013. [http://dx.doi.org/10.12989/eas.2013.4.1.085]
- [18] Y.Y. Lin, M.H. Tsai, J.S. Hwang, and K.C. Chang, "Direct displacement-based design for building with passive energy dissipation systems", *Eng. Struct.*, vol. 25, pp. 25-37, 2003. [http://dx.doi.org/10.1016/S0141-0296(02)00099-8]
- [19] T.J. Maley, T.J. Sullivan, and G. Della Corte, "Development of a displacement-based design method for steel dual systems with buckling-restrained braces and moment-resisting frames", *J. Earthquake Eng.*, vol. 14, pp. 106-140, 2010. [http://dx.doi.org/10.1080/13632461003651687]
- [20] M.J.N. Priestley, G.M., Calvi, M.J. Kowalsk, *Displacement-based design of structures.*, Istituto Universitario di Studi Superiori di Pavia: Italy, 2007.
- [21] F. Mazza, and A. Vulcano, "Displacement-based design procedure of damped braces for the seismic retrofitting of R.C. framed buildings", *Bull. Earthquake Eng.*, vol. 13, pp. 2121-2143, 2015. [http://dx.doi.org/10.1007/s10518-014-9709-7]
- [22] M. Ferraioli, and A. Lavino, "A displacement-based design method for seismic retrofit of RC buildings using dissipative braces", *Math. Probl. Eng.*, vol. 5364564, 2018. [http://dx.doi.org/10.1155/2018/5364564]
- [23] "FEMA-356 - Prestandard and commentary for the seismic rehabilitation of buildings", *Fed. Emerg. Manage. Agen.*, 2000.
- [24] *GB50011-2010 - Chinese code for seismic design of buildings.*, China Architecture & Building Press: Beijing, China, 2010.
- [25] *ASCE7-10 - Minimum design loads for buildings and other structures*, American Society of Civil Engineers, 2010.
- [26] K. Kasai, and H. Ito, "JSSI Manual for building passive control technology Part-8 peak response evaluation and design for elasto-plastically damped system", *Proceedings of 13th World Conference on Earthquake Engineering*, 2004 Vancouver
- [27] H. Ito, and K. Kasai, "Passive control design for elasto-plastically damped building structure", *Proceedings of STESSA 2006*, 2006
- [28] K. Kasai, and W. Pu, "Passive control design method for MDOF slip-hysteretic structure added with visco-elastic damper", *J. Struct. Constr. Eng.*, vol. 650, pp. 781-790, 2010. [http://dx.doi.org/10.3130/aijs.75.781]
- [29] W. Pu, and K. Kasai, "Design method for RC building structure controlled by elasto-plastic dampers using performance curve", *15th World Conference on Earthquake Engineering*, 2012 Lisbon, Portugal.
- [30] T. Takeuchi, and A. Wada, "Buckling-restrained braces and applications", In: *Japan Society of Seismic Isolation (JSSI)*, Tokyo, Japan, 2017.
- [31] M. Ferraioli, "Inelastic torsional response of an asymmetric-plan hospital building in Italy", *Proceedings of COST ACTION C26: Urban Habitat Constructions under Catastrophic Events*, 2010pp. 365-370
- [32] M. Ferraioli, D. Abruzzese, L. Miccoli, A. Vari, and G. Di Lauro, "Structural identification from environmental vibration testing of an asymmetric-plan hospital building in Italy", *Proceedings of COST ACTION C26: Urban Habitat Constructions under Catastrophic Events*, 2010pp. 981-986
- [33] M. Ferraioli, "Case study of seismic performance assessment of irregular RC buildings: Hospital structure of Avezzano (L'Aquila, Italy)", *Earthq. Eng. Eng. Vib.*, vol. 14, no. 1, pp. 141-156, 2015. [http://dx.doi.org/10.1007/s11803-015-0012-7]
- [34] *FEMA 273 - NEHRP guidelines for the seismic rehabilitation of buildings, prepared for FEMA by the applied technology council and the building seismic safety council.*, Federal Emergency Management Agency: Washington, DC, 1997.
- [35] "ATC 40 Report - Seismic evaluation and retrofit of concrete buildings", *Appl. Technol. Coun.*, 1996.
- [36] *Maual JSSI: Design and construction manual for passively controlled buildings.*, Japan Society of Seismic Isolation: Tokyo, Japan, 2007. [in Japanese]
- [37] H. Shen, R. Zhang, D. Weng, C. Gao, H. Luo, and C. Pan, "Simple design method of structure with metallic yielding dampers based on elastic-plastic response reduction curve", *Eng. Struct.*, vol. 150, pp. 98-114, 2017. [http://dx.doi.org/10.1016/j.engstruct.2017.07.047]
- [38] J. Lee, and J. Kim, "Development of box-shaped steel slit dampers for seismic retrofit of building", *Eng. Struct.*, vol. 150, pp. 934-946, 2017. [http://dx.doi.org/10.1016/j.engstruct.2017.07.082]
- [39] J. Kim, and Y. Seo, "Seismic design of low-rise steel frames with buckling-restrained braces", *Eng. Struct.*, vol. 26, no. 5, pp. 543-551, 2004.

- [40] [http://dx.doi.org/10.1016/j.engstruct.2003.11.005]
A. Teran-Gilmore, and N. Virto-Cambray, "Preliminary design of low-rise buildings stiffened with buckling-restrained braces by a displacement-based approach", *Earthq. Spectra*, vol. 25, no. 1, pp. 185-211, 2009.
- [41] [http://dx.doi.org/10.1193/1.3054638]
J. Kim, H. Choi, and L. Chung, "Energy-based seismic design of structures with buckling-restrained braces", *Steel Compos. Struct.*, vol. 4, no. 6, pp. 437-452, 2004.
- [42] [http://dx.doi.org/10.12989/scs.2004.4.6.437]
H. Choi, and J. Kim, "Energy-based seismic design of buckling-restrained braced frames using hysteretic energy spectrum", *Eng. Struct.*, vol. 28, no. 2, pp. 304-311, 2006.
- [43] [http://dx.doi.org/10.1016/j.engstruct.2005.08.008]
A. Habibi, R.W.K. Chan, and F. Albermani, "Energy-based design method for seismic retrofitting with passive energy dissipation systems", *Eng. Struct.*, vol. 46, pp. 77-86, 2013.
- [44] [http://dx.doi.org/10.1016/j.engstruct.2012.07.011]
L.F.F. Miguel, and R.H. Lopez, "Robust design optimization of friction dampers for structural response control", *Struct. Contr. Health Monit.*, vol. 21, no. 9, pp. 1240-1251, 2014.
- [45] [http://dx.doi.org/10.1002/stc.1642]
C.A. Martínez, O. Curadelli, and M.E. Compagnoni, "Optimal placement of non-linear hysteretic dampers on planar structures under seismic excitation", *Eng. Struct.*, vol. 65, pp. 89-98, 2014.
- [46] [http://dx.doi.org/10.1016/j.engstruct.2014.01.030]
Y. Terazawa, and T. Takeuchi, "Optimal damper design strategy for braced structures based on generalized response spectrum analysis", *J. Struct. Constr. Eng.*, vol. 83, no. 753, pp. 1689-1699, 2018.
- [47] [http://dx.doi.org/10.3130/aijs.83.1689]
T. Takeda, M.A. Sozen, and N.N. Nielsen, "Reinforced concrete response to simulated earthquakes", *J. Struct. Div.*, vol. 96, no. 12, pp. 2557-2573, 1970.
- [48] [http://dx.doi.org/10.1061/JSDEAG.0002765]
"NTC-2018 Guidelines - Technical standards for constructions", *Off. J. Italian Repub. Circ.*, Rome, Italy, 2018. (in Italian).
- [49] "NTC-Instructions - Instructions for the application of the new technical norms on constructions", *Off. J. Italian Repub. Circ.*, vol. 7, 2019. (in Italian).
- [50] *EN 1998-3:2005 - Comité Européen de Normalisation CEN, Eurocode 8 - Design of structures for earthquake resistance - Part 3: Assessment and retrofitting of buildings*, European Communities for Standardization, Brussels, Belgium, 2005.
- [51] "CSI Computer & Structures Inc. SAP2000. Linear and non-linear static and dynamic analysis of three-dimensional structures", In: *Research Ultimate Version 21.0, Analysis Ref. Manual, Computer and Structures*, Berkeley, CA., 2019.
- [52] J.B. Mander, M.J.N. Priestley, and R. Park, "Theoretical stress-strain model for confined concrete", *J. Struct. Eng.*, vol. 114, no. 8, pp. 1804-1826, 1988.
- [53] [http://dx.doi.org/10.1061/(ASCE)0733-9445(1988)114:8(1804)]
Y.K. Wen, "Method of random vibration of hysteretic systems", *J. Eng. Mech.*, vol. 102, no. 2, pp. 249-263, 1976.
- [54] I. Iervolino, C. Galasso, and E. Cosenza, "REXEL: computer aided record selection for code-based seismic structural analysis", *Bull. Earthquake Eng.*, vol. 8, pp. 339-362, 2010.
- [55] [http://dx.doi.org/10.1007/s10518-009-9146-1]
C. Smerzini, and R. Paolucci, *Research Project DPC - RELUIS 2010-2013, SIMBAD: a database with selected input motions for displacement-based assessment and design - 2nd release.*, Department of Structural Engineering: Politecnico di Milano, Italy, 2011.
- [56] M.N. Fardis, *Seismic Design, assessment and retrofitting of concrete buildings.*, Springer, 2009.
- [http://dx.doi.org/10.1007/978-1-4020-9842-0]